University of Kentucky Master's Theses   Graduate School

2010

CORRELATING THE MAGNITUDE AND SPATIAL GRADIENT OF ALTERNANS

Stuart Traxel
University of Kentucky, straxel@gmail.com

ABSTRACT OF THESIS

CORRELATING THE MAGNITUDE AND
SPATIAL GRADIENT OF ALTERNANS

Electrical restitution has been shown to inaccurately predict the occurrence of alternans
of action potential duration. A new method using the spatial gradient of alternans (SGA)
is proposed to predict alternans and cardiac electrical stability. A simulated 1-D strand of
tissue was used to compare indexes computed from restitution methods and the SGA
method to changes in the amplitude of alternans using different electro-physiological
alterations. The SGA method correlated better with changes in the amplitude of alternans
than restitution methods for a decrease in the transient outward current (I_{to}) and
conduction velocity. Restitution methods correlated better with changes in the amplitude
of alternans than the SGA method when the inward rectifier potassium current (I_{k1}) and
the delayed rectifier potassium current (I_{kr}) were decreased. Restitution methods and the
SGA method correlated well with changes in the amplitude of alternans when the L-type
calcium channel current (I_{CaL}) was altered and when I_{kr}, I_{k1}, and the sodium/calcium
exchange current (I_{NaCa}) were increased. The SGA method includes the effect of
conduction in tissue and reveals other features that provide advantages in predicting
stability over currently used restitution methods.

KEYWORDS: Cardiac electrical stability, electrical restitution, sudden cardiac death,
alternans, conduction velocity

<u>Stuart Traxel</u>
<u>04/30/2010</u>

CORRELATING THE MAGNITUDE
AND SPATIAL GRADIENT OF ALTERNANS

By

Stuart Traxel

Dr. Abhijit Patwardhan
Director of Thesis

Dr. Abhijit Patwardhan
Director of Graduate Studies

04/30/2010

RULES FOR THE USE OF THESES

Unpublished theses submitted for the Master's degree and deposited in the University of Kentucky Library are as a rule open for inspection, but are to be used only with due regard to the rights of the authors. Bibliographical references may be noted, but quotations or summaries of parts may be published only with the permission of the author, and with the usual scholarly acknowledgments.

Extensive copying or publication of the thesis in whole or in part also requires the consent of the Dean of the Graduate School of the University of Kentucky.

A library that borrows this thesis for use by its patrons is expected to secure the signature of each user.

Name   Date

_____

_____

_____

_____

_____

_____

_____

_____

_____

THESIS

Stuart Traxel

The Graduate School

University of Kentucky

2010

CORRELATING THE MAGNITUDE AND SPATIAL GRADIENT OF ALTERNANS

_____

THESIS

_____

A thesis submitted in partial fulfillment of the
requirements for the degree of Master of Science
in Biomedical Engineering in the Graduate School
at the University of Kentucky

By

Stuart Traxel

Lexington, Kentucky

Director: Dr. Abhijit Patwardhan, Professor of Biomedical Engineering

Lexington, Kentucky

2010

DEDICATION

This thesis would not be possible without the constant love and support of my family.

ACKNOWLEDGEMENTS

TABLE OF CONTENTS

LIST OF TABLES

LIST OF FIGURES

LIST OF FILES

Chapter One: Introduction

Sudden cardiac deaths (SCD) comprise the majority of the cardiac disease deaths and are estimated to occur in more than 300 000 people each year within the United States [1, 2]. T-wave alternans, a beat-to-beat variation in the T-wave, is considered to increase the risk of the development of arrhythmic activity, [3, 4] which can lead to sudden cardiac death. Alternation of the T-wave is a result of the repolarizing phase of the action potential duration (APD) alternating from beat-to-beat.

The slope of electrical restitution has been used to predict the onset of alternating APD values [5, 6], hereafter known as APD alternans. Restitution has been defined in this sense as a function of APD on the preceding diastolic interval (DI). Restitution curves have been constructed using the DI as the independent variable and the APD as the dependent variable. Steep restitution curves have been linked to spiral wave break up at the tip [7, 8] and the onset of alternans [5, 6], furthering the idea that alternans is an underlying mechanism of arrhythmic activity.

Nolasco and Dahlen originally proposed the restitution hypothesis by theorizing a dependence of APD on the preceding DI, and stating that when the slope of this relationship is ≥1, alternans will occur [5]. Protocols, such as standard and dynamic restitution, have since been developed to compute APD based upon the preceding DI [9]. The standard restitution protocol was developed to measure restitution for intermittent beats of variable length. Studies later showed that other effects, including cardiac memory [10-12], influence whether alternans occur and consequently that a unity slope in the standard restitution curve does not predict the occurrence of alternans [9, 12]. As a result, the dynamic restitution protocol was developed to evaluate the importance of cardiac memory during pacing [9].

In addition to cardiac memory, heterogeneities such as conduction velocity (CV) restitution can cause discordant alternans, which is considered unstable behavior [13, 14]. Restitution of CV is one mechanism of discordant alternans [14], where APD varies spatially as well as temporally, which is thought to be proarrhythmic [15]. Memory and

CV restitution are examples of other mechanisms that can influence the occurrence of alternans. Several studies have shown that a restitution slope ≥1 does not predict the onset of alternans [16-18] and that the maximum restitution slope is not related to the magnitude of alternans [19]. Restitution is not necessary for alternans to occur [20], confirming that APD is not just a function of the previous DI. Restitution therefore has effects both independent and dependent upon DI. Both the DI independent and DI dependent mechanisms of alternans are seen when pacing at constant cycle lengths (CL) when alternans occurs. A novel pacing protocol that can pace at a constant DI [20, 21], allows analysis of the mechanism of alternans that is independent of DI. Analyzing restitution effects that are dependent on only DI is therefore not possible when pacing in a single cell since there is no pacing method that can study only the restitution effects that are dependent of DI.

Instead, the DI dependent mechanism of alternans can be studied by pacing in tissue. By pacing at a constant DI at one end of the tissue and allowing activations to travel to the other end of tissue where DI alternates, two sections of tissue are studied, one with and one without DI dependence. The difference between these two sections of tissue is quantified to obtain a measure of restitution that is DI dependent only, hereafter known as the spatial gradient of alternans (SGA) because of the gradual increase of APD alternans seen progressing away from the pacing site. The SGA method, unlike restitution, also shows how alternans changes spatially and provides us with a method to predict how spatial effects influence stability. The SGA method is therefore hypothesized to predict changes in stability better than restitution methods. This study proposes the SGA method as a method of predicting cardiac electrical stability and will evaluate how well the SGA method and restitution methods correlate with a particular measure of stability.

Chapter Two: Background

Electrical function of the heart:

The function of the heart is to pump blood to the body. Electrical conduction throughout the heart causes the mechanical contraction of the heart which pumps blood to the body. Electrical conduction begins at the sinoatrial node, the pacemaker of the heart, where electrical impulses are generated. Electrical impulses first flow to the atria, causing the atria to contract and pump blood into the ventricles. The atrioventricular (AV) node, the pathway used to conduct electrical impulses from the atria to the ventricles, delays conduction to allow the ventricles to fill with blood. After a short delay, conduction passes from the Bundle of His to the right and left bundle branches in each ventricle, and then spreads out to the Purkinje fibers and ends in ventricle contraction. Conduction from the AV node to the Purkinje fibers is very rapid, on the order of 0.5 m/s, causing the ventricles to contract nearly simultaneously [22].

Cardiac electrical stability:

Cardiac electrical stability is a broad term referring to the likelihood that electrical activations throughout the heart will become abnormal and cause lethal arrhythmic activity. A loss of cardiac electrical stability can induce unstable behavior such as tachycardia and fibrillation, which can lead to sudden cardiac death [23]. Alternans has since been considered a marker of arrhythmic activity [3] and cardiac electrical instability [23]. Simulations have shown alternans causing wavefronts of electrical activity to fracture [7]. This unstable behavior can cause reentry mechanisms to develop and propagate throughout the myocardium.

Electrocardiogram and T-wave alternans:

The electrocardiogram (ECG) is a measurement tool that shows electrical activity of the heart over a given time interval. Figure 1 shows an example of an ECG tracing. The P, QRS, and T waves labeled in Figure 1 correspond to atria depolarization, ventricle depolarization, and ventricle repolarization respectively. During the T-wave, ventricular myocytes begin to repolarize (discussed in the next section as phase 3 in Figure 2), which collectively contribute to produce the T-wave in Figure 1. Alternans in the T-wave occur when the T-wave varies in amplitude or shape during alternating beats. This beat-to-beat variation of the T-wave occurs when the APDs of myocytes repolarize in an alternating long-short fashion. A T-wave alternans test has been developed to determine whether a patient is vulnerable for arrhythmic activity [24].
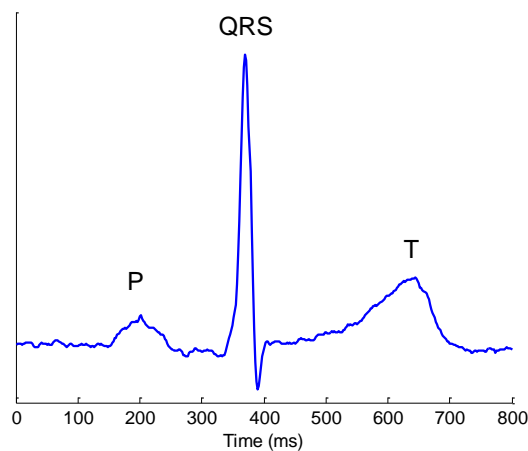
Figure 1, ECG tracing showing the location of P, QRS, and T waves.

Cardiac action potential:

Cardiac action potentials occur in myocytes and propagate throughout the heart to allow it to properly contract. The five phases of a cardiac action potential are labeled in Figure 2. Phase 4 corresponds to the DI and is when the myocyte is at its resting potential. Phase 0 is when the cell depolarizes and a rapid influx of Na^+ ions enter the myocyte. A notch in the action potential occurs during phase 1. It can be attributed to the closing of

the Na^+ channels and a brief contribution of the transient outward K^+ current. A plateau initially forms during phase 2, as L-type calcium enters the cell, while potassium currents, such as I_{kr} and I_{k1} cause potassium to leave the cell. Phase 3 is when the cell repolarizes and returns to resting potential. During this phase, the L-type calcium channels close and K^+ channels stay open causing a sharp decrease in membrane voltage until the cell is fully repolarized to its resting potential. The contributions of the five ionic currents studied are shown in Figure 3. Phases 0-3 roughly correspond to the APD or the systolic period when the myocyte contracts, while phase 4 corresponds to the DI or when the heart is not contracting. The length of APD is quantified differently to according to the application. Quantifying APD as 90% of repolarization is common when taking into account all systolic activity.
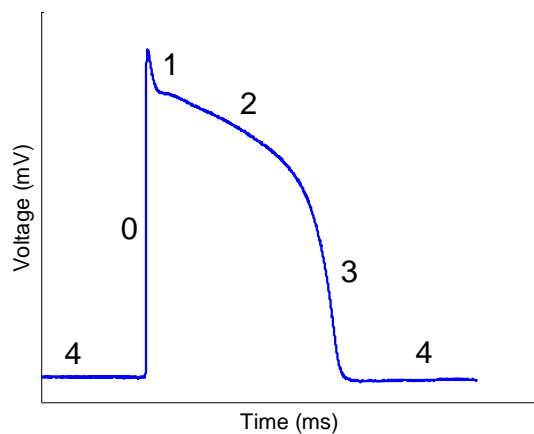
Figure 2, Cardiac action potential of a myocyte. Phases 0-4 represent depolarization, the notch and initial repolarization of the AP, the plateau phase, rapid repolarization, and the cell at rest respectively.

A
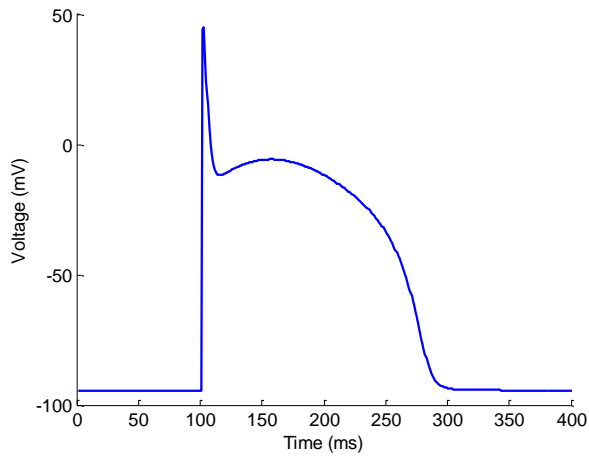
B
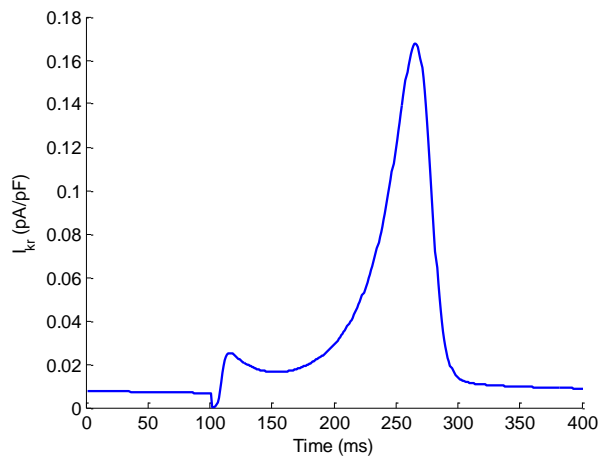
Figure 3, The (A) simulated action potential and underlying ionic currents: (B) I_{kr}, (C) I_{k1}, (D) I_{to}, (E) I_{CaL}, and (F) I_{NaCa}, which among other ionic currents sum to produce the simulated action potential.

C
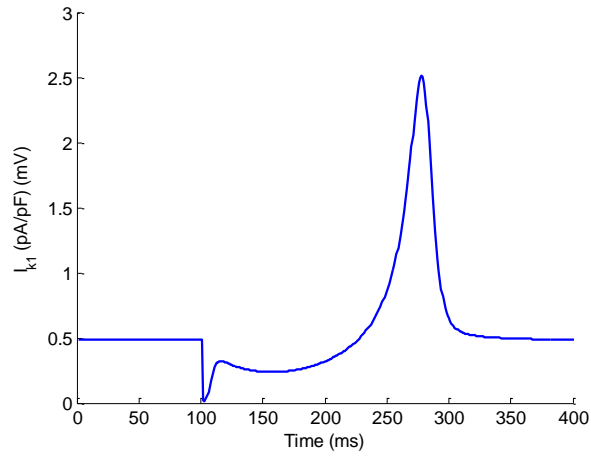
D
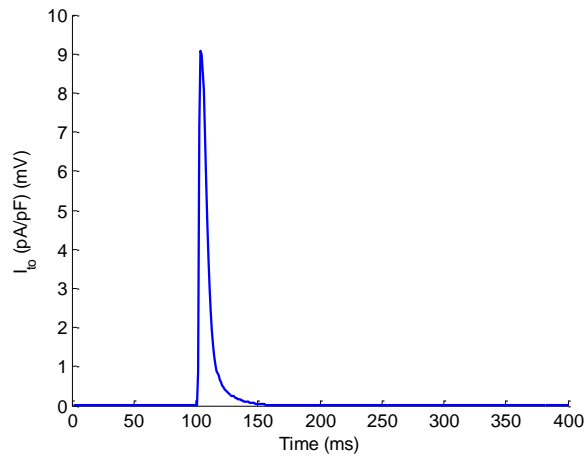
Figure 3, continued. The (A) simulated action potential and underlying ionic currents: (B) I_{kr}, (C) I_{k1}, (D) I_{to}, (E) I_{CaL}, and (F) I_{NaCa}, which among other ionic currents sum to produce the simulated action potential.

E
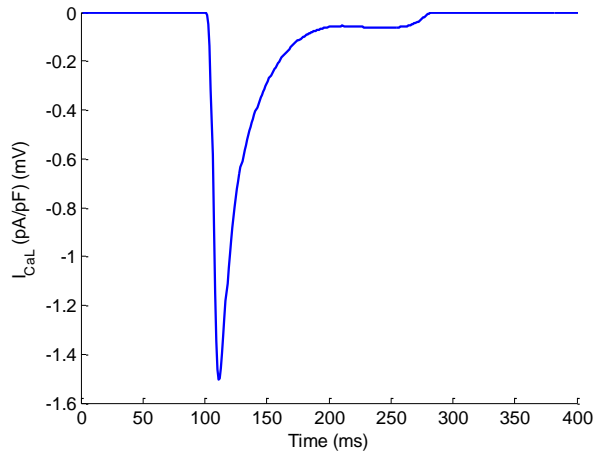
F
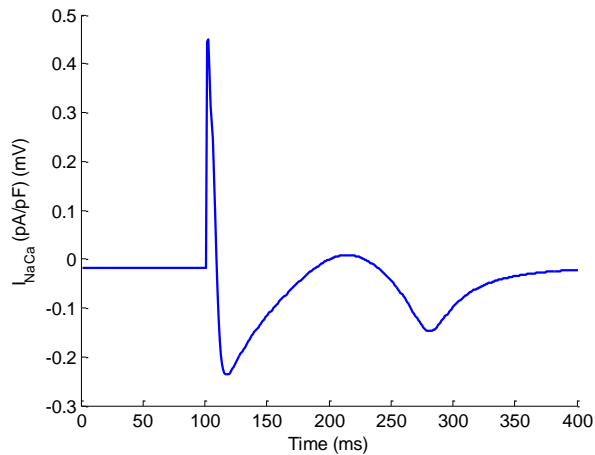
Figure 3, continued. The (A) simulated action potential and underlying ionic currents: (B) I_{kr}, (C) I_{k1}, (D) I_{to}, (E) I_{CaL}, and (F) I_{NaCa}, which among other ionic currents sum to produce the simulated action potential.

Electrical restitution:

As stated before, electrical restitution relates an APD with the preceding DI. Pacing at shorter intervals causes both DI and APD to shorten. Values of APD and DI must shorten at higher heart rates to ensure conduction block does not occur. Values of APD and DI are obtained at different pacing intervals to compute restitution curves, which

show the relationship between APD and DI at each pacing interval. Nolasco and Dahlen were the first to predict that when a restitution curve had a slope greater than 1, values of APD would alternate in a long-short fashion, which is referred to as APD alternans [5]. Since alternans has been proposed to predict cardiac electrical stability [3, 23], the slope of restitution curves have been subsequently used to predict the occurrence of alternans and unstable behavior. A slope >1 during restitution has been theorized to induce spiral wave breakup [7, 8], which has been considered analogous to the transition from tachycardia to fibrillation. Figure 4 shows an example of the restitution curve.
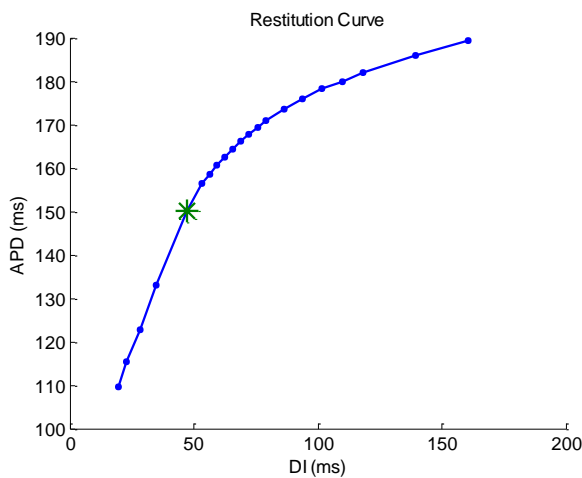
Figure 4, A sample restitution curve. Notice the steep slopes at short values of DI and shallow slopes at higher values of DI. The asterisk represents where the slope equals unity.

Restitution of APD can be measured using different protocols. Each protocol expresses different cardiac dynamics and explores different situations in which arrhythmia could be induced. Standard and dynamic restitution protocols are two of the most common protocols used to measure APD restitution.

The standard restitution protocol delivers a variable S2 stimulus after a train of S1 stimuli with fixed CLs used to reach steady state. This protocol predicts the effect of an ectopic beat during sinus rhythm. Mendez et al. published the first restitution curve using a

protocol similar to the the standard restitution protocol by pacing for six beats to achieve steady state followed by a premature beat [25].

After studies found that the accumulation of memory affects restitution [10-12], Koller et al. developed the dynamic restitution protocol to take this effect into account [9]. The dynamic restitution protocol delivers a train of S1 beats at a fixed CL, with each train of beats being at a different CL. Values of APD and DI for the last beat at the end of each train are computed to acquire a restitution curve. Unlike the standard protocol, the dynamic protocol takes into account the accumulation of memory on restitution by rapidly pacing at the same CL.

Conduction velocity restitution:

Conduction velocity slows for very short DIs which leads to a functional relationship between DI and CV and can cause CV to alternate for alternating beats. By slowing CV during rapid pacing, the distance between the current and the previous wavefront of activation will increase. When pacing intervals are repeatedly short, APD may vary spatially as a result of CV restitution which can cause unstable behavior such as discordant alternans. Spiral wave breakup has been shown in simulations to occur away from the spiral wave tip as a result of CV restitution and discordant alternans [7]. When a wavefront of activation slows down, if the following wave of activation does not slow down at an equal or greater velocity, block can occur. If block occurs in some regions of the wavefront and not others, reentry can occur around this heterogeneity and disperse throughout the tissue [7].

Concordant and discordant alternans:

In discordant alternans, APD varies spatially and temporally, while APD varies only temporally in concordant alternans. Discordant alternans is considered more likely to produce TWA than concordant alternans [15]. Discordant alternans is hypothesized to require heterogeneity, such as a tissue heterogeneity [14], CV restitution [13, 14], or

short-term memory [13] to occur. During discordant alternans, APD alternates with opposite phase from beat-to-beat as the wavefront propagates through tissue as shown in Figure 5.
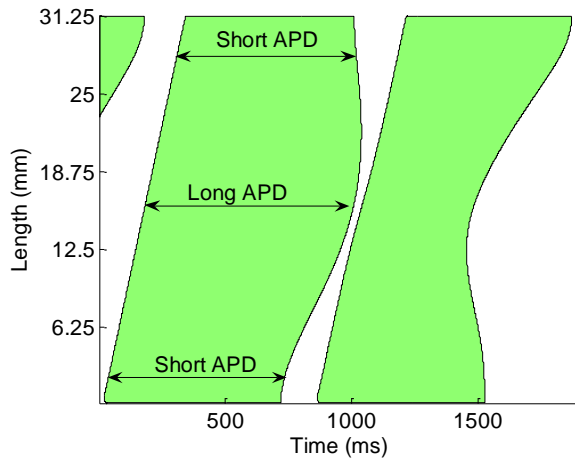
Figure 5, Space-time plot showing discordant alternans for two beats in a 1-D strand of tissue. Green represents APD and white represents DI. Notice how APD varies for different cells in the tissue.

Mathematical modeling:

Action potentials are modeled by summing underlying ionic currents. Membrane voltage is considered to have both capacitive and non-capacitive effects. Hodgkin and Huxley modeled the axon in giant squid using a constant capacitance in Equation 1 [26]. In Equation 1, V_m is membrane voltage, C_m is membrane capacitance, and I_i is the ionic current density. The integral of I_i is typically denoted as $\sum_i I_i$ and represents the sum of individual ionic currents within the cell. As complex features of cellular properties have been discovered, additional ionic currents have been incorporated into detailed models to more accurately depict myocyte behavior.

$$V_m = \frac{-1}{C_m} * \int I_i$$

Equation 1. The Hodgkin-Huxley model is used to simulate neuron activation and propagation.

The canine ventricular myocyte model (CVM), which has a total of 13 variables and 10 gates, is used in this study to examine cardiac dynamics [27]. The equation used to compute transmembrane potential for the CVM model is listed below [27]. Equations for the 13 ionic currents that comprise the model can be found in Appendix 2. Diffusion is used to compute the propagation of voltage in tissue shown in Equation 2 [28].

$$\frac{\partial v}{\partial t} \approx -(I_{stim} + I_{Na} + I_{K1} + I_{Kr} + I_{Ks} + I_{to} + I_{Kp} + I_{NaK} + I_{NaCa} + I_{Nab} + I_{Cab} + I_{pCa}$$
$$+ I_{Ca} + I_{Cak} + D_x * \frac{v(x + \Delta x) - 2 * v(x) + v(x - \Delta x)}{(\Delta x)^2}$$

Equation 2. The sum of 13 ionic currents and a stimulus current compute voltage in time for the CVM model. Diffusion is used to compute voltage in space, where Δx is the simulated distance between two cells and D_x is the diffusion coefficient.

Controlling the value of diastolic interval:

Studies have been published where the value of DI has been controlled while pacing cardiac tissue [20, 21]. By controlling DI, the effect of restitution and other mechanisms can be analyzed within cardiac tissue. The value of DI is controlled by computing the voltage in real-time and determining when the action potential is 90% repolarized, referred to as APD_{90}. When the action potential is 90% repolarized, a stimulus will be delivered after a specified time. This specified time is the DI preceding the following stimulus.

Chapter Three: Methods and Analysis

The canine ventricular model (CVM) developed by Fox et al [27] was used to simulate electrical activation in cardiac tissue. The CVM model was used because of its complexity and because it can induce APD alternans when DI is controlled at a constant value from beat to beat. The programming language used to implement the CVM model was FORTRAN95. The operator splitting method was used to make computations separately in time and space. Diffusion was used to simulate isotropic propagation across the tissue. The fifth-order Runge Kutta time stepping scheme was used to compute transmembrane voltage for each time step. The time steps used were 0.1 and 0.001 ms for the adaptive time step method. Values of voltage were stored every 0.2 ms to reduce the size of files that were stored for each simulation. The distance between simulated cells was 125 μm with a diffusion constant of 0.0007 cm^2/s, since a diffusion constant 0.001 cm^2/s used by Cherry [29] did not allow propagation of stimuli throughout the tissue for simulations. The length of tissue was simulated as 250 cells, or 31.25 mm. Stimuli given were -280 μA/μF in tissue and -80 μA/μF in a single cell. Stimuli were given at twice the diastolic threshold using the minimum CL at which conduction block does not occur. All simulations were initially paced for 200 beats, each with duration of 500 ms, to obtain steady state.

Different electro-physiological alterations were performed to examine how the SGA, standard restitution, and dynamic restitution changed for each alteration. In the CVM model, the following ionic currents were altered; the L-type calcium current (I_{CaL}) by ±5%, the transient outward current (I_{to}) by ±10%, the inward rectifier potassium current (I_{k1}) by ±7%, the rapid component of the delayed rectifier current (I_{kr}) by ±62%, and the sodium-calcium exchange current (I_{NaCa}) by ±50%. These alterations were chosen because a 5% decrease in I_{CaL}, a 10% increase in I_{to}, a 7% increase in I_{k1}, a 62% increase in I_{kr}, and a 50% decrease in I_{NaCa} eliminated alternans in a single cell [27]. The effect of changing CV was computed by altering CV by ±5%. The diffusion coefficient (D_x) was changed by an amount that would alter CV by ±5%. The value of CV was decreased to

0.452 m/s and increased to 0.5 m/s from a control CV of 0.476 m/s to alter CV by ±5%. Table 1 shows the alterations that were made in this study.

Table 1, List of electro-physiological alterations used. The ionic current alterations were chosen because they eliminated alternans in a single cell [27]. A 5% change in CV was chosen because altering CV by ±10% would not allow conduction in the tissue.

Ionic Current	Alteration Amount
I_{kr}	±62%
I_{k1}	±7%
I_{to}	±10%
I_{CaL}	±5%
I_{NaCa}	±50%
CV	±5%

Dynamic and standard restitution curves were computed for each electro-physiological alteration. Each restitution protocol was paced at a site that was 0.625 mm from the end of the simulated tissue (cell 5) using parameters shown in Appendix 1. A distance of 0.625 mm from the end of the tissue was selected to account for the effects that Von Neumann boundary conditions have on either end of a simulated 1-D tissue strand. The dynamic restitution curve was obtained using trains of 50 S1 stimuli at variable CLs. Cycle lengths were decreased in steps of 25 ms from 350 ms to 300 ms, decreased in steps of 10 ms from 290 ms to 250 ms, and decreased in steps of 5 ms from 245 ms until conduction block was reached [9]. The APD following the 50th stimulus and the DI preceding the 50th stimulus in each S1 train were the values of APD and DI used in the dynamic restitution curve. Standard restitution curves were obtained by delivering a S2 stimulus after 20 S1 stimuli with cycle lengths (CL) of 300 ms in tissue. The S2 stimuli that were delivered were decremented by 5 ms, starting at 300 ms and ending when 2:1 conduction block was reached [9]. The APD following the S2 stimulus and the DI preceding the S2 stimulus in each S1 train were the values of APD and DI used in the standard restitution curve. Each restitution curve was fit to an exponential function. The sum of APD and DI was computed for the fitted exponential function at a point at which the slope was equal to unity. If a point could not be found where the slope was equal to

unity, the sum of APD and DI was computed at a point where the slope approached +1. The sum of APD and DI at this point was used as the index of stability for each electro-physiological alteration.

The SGA method was computed by pacing at a site 0.625 mm away from the end of the simulated tissue (cell 5) for 151 beats and using 35 ms values of DI. Values of DI were chosen to induce alternans in tissue without causing conduction block at sites distal to the pacing site. Steady state was acquired by pacing the tissue for 151 beats [14]. The value of DI was controlled at the pacing site by identifying where APD_{90} is in "real time" and then waiting for 35 ms until the next stimulus was delivered [20, 21]. The amplitude of APD alternans was computed as the absolute difference between the APDs of the last two beats for each cell. The values of APD alternans were low pass filtered using a digital Butterworth filter with a cutoff frequency of 0.06 Hz to filter noise out of the SGA curve. The index computed from the SGA was computed as the slope of a line connecting the amplitude of alternans at the pacing site to a site distal to the pacing site where the amplitude of alternans peaked.

The amplitude of alternans was computed for each electro-physiological alteration to serve as a measure of cardiac electrical stability. The amplitude of alternans was computed when pacing at a 200 ms CL during the dynamic protocol, since these simulations were already used to acquire the dynamic restitution curve. The absolute difference of the APD values following the 49th and 50th stimuli when the pacing CL was 200 ms were used to compute the amplitude of alternans.

Percent changes were used to quantify how much an electro-physiological alteration had changed the value of an index in order to compare all three methods and changes in the amplitude of alternans. Percent changes were computed between the index computed during control and the index computed after an electro-physiological alteration had been made for each method and the amplitude of alternans. Percent changes were compared between the three methods and the amplitude of alternans to determine how each method correlated with changes in the amplitude of alternans for each particular electro-

physiological alteration. A method was considered to correlate well if its percent change had the same sign as the percent change of the amplitude of alternans for the same electrophysiological alteration. A method did not correlate well if its percent change had a different sign as the percent change of the amplitude of alternans for the same electrophysiological alteration.

Baseline APDs were computed at CLs of 350 ms and 200 ms for each electro-physiological alteration. Simulations used to compute the dynamic restitution curve were used to compute baseline APD values during steady state. Baseline APDs were computed as the average of the APDs following the 49th and 50th stimuli of the two respective S1 trains (when CL was 350 ms and 200 ms) to account for the occurrence of alternans at shorter values of CL.

Restitution curves were computed using DI control and CL control pacing protocols when no electro-physiological alterations were made and when I_{kr} was decreased. These restitution curves were computed to explain results that occurred when I_{kr} was decreased. Simulations controlling CL used the dynamic protocol as described earlier. Simulations that used DI control used trains of 50 beats and started at a DI value of 150 ms. After pacing for 50 beats at a constant DI of 150 ms, DI was decremented by 25 ms for another 50 beat train. This process was repeated until DI was equal to 100 ms. At this point, DI was decremented in steps of 5 ms after each 50 beat train until DI was equal to 35 ms. A single cell was used to compute restitution curves when evaluating the difference between DI control and CL control since DI control is designed to control the value of DI only for a particular cell.

Indexes were computed from the SGA method when DI was controlled at values of 30, 35, and 40 ms. The value of DI was changed to examine the effect that changing pacing intervals would have on the index computed from the SGA method.

Conduction velocity (CV) restitution was computed using DI control. Computing CV restitution using DI control better depicts the effect CV restitution has on indexes computed from the SGA method, since the SGA method uses DI control for simulations.

Restitution of CV was computed using a protocol similar to the dynamic protocol, except DI was controlled and not CL. Trains of 50 beats were used for each value of DI. After 50 beats of a DI controlled at 50 ms, DI was decremented by 2 ms and then paced for another 50 beats. This process was repeated until DI was equal to 30 ms. The values of DI used for the CV restitution curve was the last DI of each S1 train in the middle of the tissue. The values of CV used for the CV restitution curve was the CV of the last beat of each S1 train between the pacing site and the middle of the tissue.

The process used to compute each index of stability will be detailed further in the Results section. Values of APD and DI were computed for each simulation using a custom program written in MATLAB.

Chapter Four: Results

Figure 6 illustrates the process used to compute a value that serves as an index of stability for the SGA method. In the SGA method, DI was controlled at a short constant value during pacing at one end of the tissue which led to DI and APD alternating at an increasing rate away from the pacing site. Figure 6A shows the pacing site, where DI is constant, and a site in the middle of the tissue, where DI is not constant. The value of DI was not controlled in the middle of the tissue, which caused DI to alternate. Increasing DI alternation caused an increase in APD alternation as a result of APD restitution.

Figure 6B is a space-time plot of beats 148-151 during simulation. Again notice how DI and APD alternate more at sites increasingly further from the pacing site, at which DI is controlled. The target DI was 35 ms for each beat at the pacing site. Computed DI values were an average 1.5 ms less than the target DI, but DIs remained relatively constant beat by beat, varying by ± 0.1 ms.

Figure 6C shows how APD varies spatially throughout the tissue for the 150th and 151st beats. The absolute difference was taken between the values of APD for the 150th and 151st beats to compute APD alternans for each cell. Figure 6D shows APD alternans values at each cell after the SGA curve was low-pass filtered. Low-pass filtering APD alternans values using a cutoff of 0.06 Hz changed APD alternans values from the pacing site to the end of the tissue by less than 5%. Low-pass filtering removed noise and smoothed the SGA curve in Figure 6D to reduce the error involved when computing the indexes of stability of the SGA method. Without the low pass filter, the site at which APD alternans peaked changed enough to affect the index computed from the SGA method. A line was fit from the pacing site to the site at which APD alternans peaked to compute the index of stability in the low-pass filtered curve. The slope of this fitted line served as an index of stability computed from the SGA.

18

A
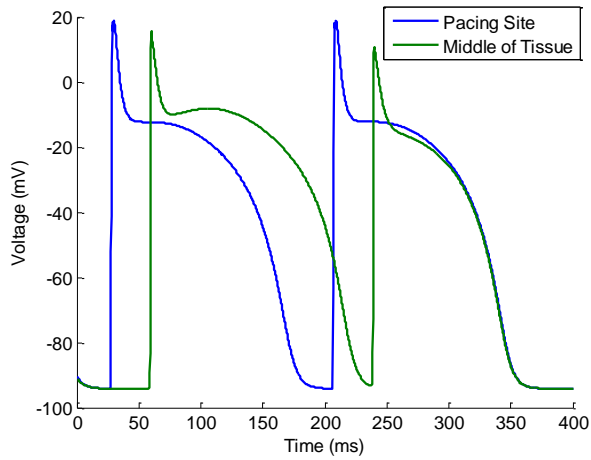
B
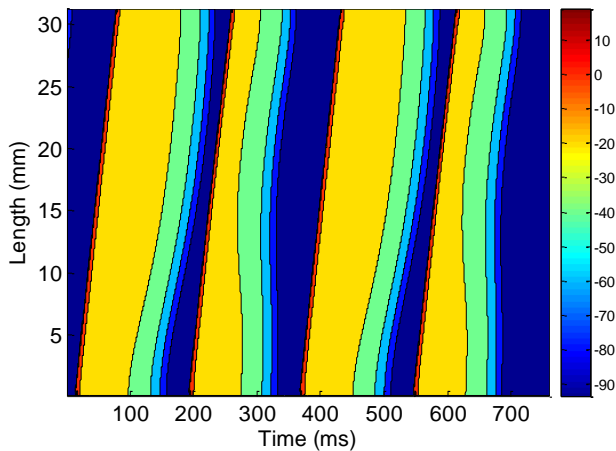
Figure 6, Development of the SGA. (A) Simulated transmembrane potentials (TMPs) of the pacing site, where DI is held constant, and a site in the middle of the tissue where DI is not constant. (B) A space-time plot of simulated TMPs for the last four beats of the protocol. More positive TMPs are in lighter color and more negative TMPs are in darker color - see color key. (C) The spatial distribution of APD for the last two beats. (D) The absolute difference of APD alternans for the last two beats at each cell. The index used to predict stability for the SGA method is the slope of the linear fit.

C

D
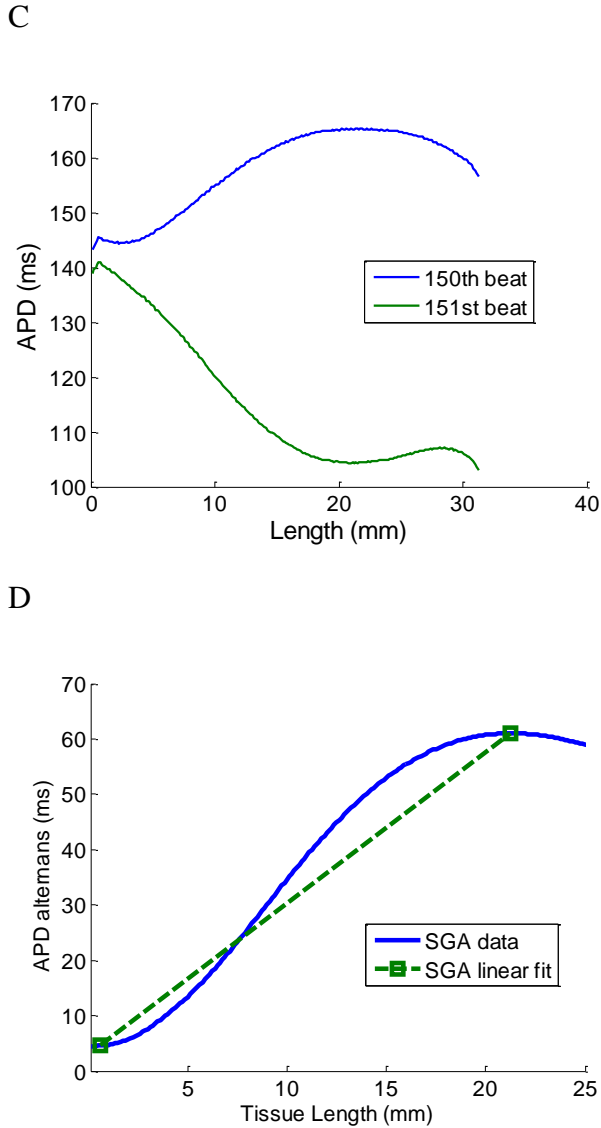
Figure 6, continued. Development of the SGA. (A) Simulated transmembrane potentials (TMPs) of the pacing site, where DI is held constant, and a site in the middle of the tissue where DI is not constant. (B) A space-time plot of simulated TMPs for the last four beats of the protocol. More positive TMPs are in lighter color and more negative TMPs are in darker color - see color key. (C) The spatial distribution of APD for the last two beats. (D) The absolute difference of APD alternans for the last two beats at each cell. The index used to predict stability for the SGA method is the slope of the linear fit.

Figure 7 shows what happened when DI was controlled at different pacing intervals. At shorter pacing intervals, the site where APD alternans peaked moved closer to the pacing

site. The value of APD alternans at the site where APD alternans peaked also increased, which increased the index computed from the SGA method. At longer pacing intervals, the value of APD alternans at the site at which APD alternans peaked decreased and the site moved further away from the pacing site, which decreased the index computed from the SGA method. Mechanisms that affect the site at which APD alternans peaked should also have a similar affect on the APD node, a site in the tissue where two consecutive beats have equal values of APD. Watanabe et al. state that CV restitution affects the position of the APD node [14], and should therefore also affect the site where APD alternans peaked. This will be explained further in the discussion section.
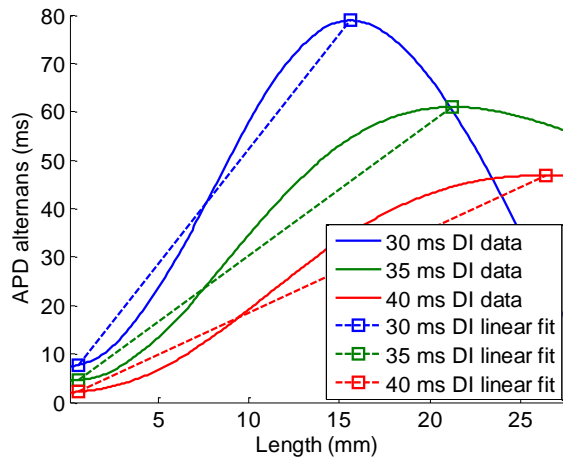
Figure 7, Computation of SGA when paced at different values of DI. Pacing at shorter intervals increased indexes computed from the SGA more than any other electro-physiological alteration studied.

Figure 8 shows conduction velocity (CV) restitution. For sites further away from the pacing site, DI alternates more and shorter DIs entered the steep portion of the CV restitution curve. The value of CV decreased for these short values of DI. Shorter pacing intervals engaged CV restitution for sites closer to the pacing site. CV restitution is one factor besides restitution that can influence stability.
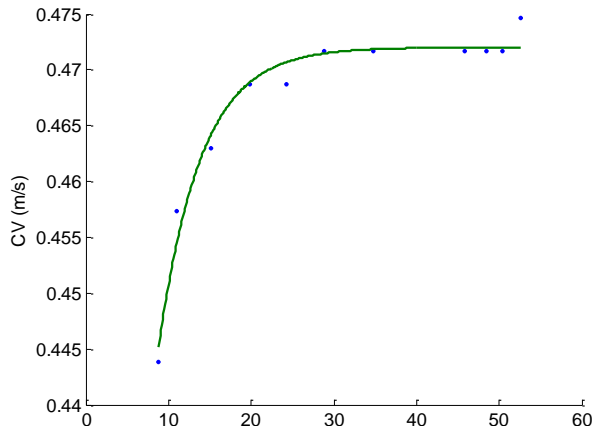
Figure 8, Conduction velocity (CV) restitution during DI control. Restitution of CV was fit by the equation $CV = a + b * \exp(DI / c)$ where $a=0.472$, $b=-0.147$, $c=5.18$, and $r^2 = 0.98$.

Indexes were computed to predict changes in stability for standard and dynamic restitution protocols. After restitution curves were simulated, restitution curves were fit with an exponential function. All exponential functions used to fit restitution curves had an r^2 value ≥ 0.99. Indexes were computed using the values of APD and DI at a point when the exponential function fit to the restitution curve had a slope that approached +1. Figure 9 shows the point at which the slope approaches +1 and the APD and DI values at this point. The values of APD and DI at this point were summed to represent an index of stability for both restitution methods.
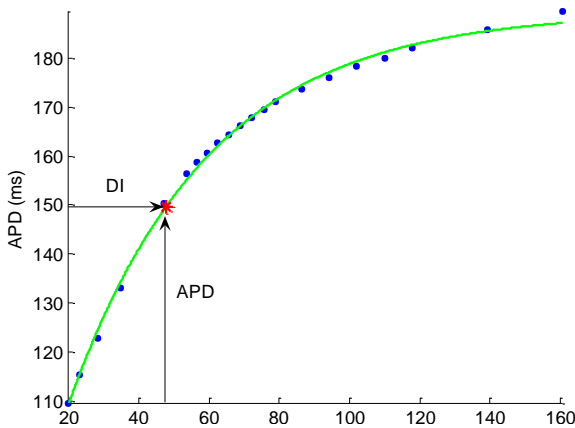
Figure 9, Computing the index of stability used for restitution methods. The restitution curve was fit with an exponential function APD = a + b * exp(DI / c). The location at which the slope approached +1 was computed for the fitted exponential function. The values of APD and DI at this location were summed to give an index of stability of the restitution methods for each electro-physiological alteration.

Table 2 shows the values of the amplitude of APD alternans during a pacing CL of 200 ms, which were used as a measure of stability. Percent changes were computed for each electro-physiological alteration. In Table 2, the resultant 83.2% percent change when I_{kr} was decreased by 62% was computed by calculating the percent change between alternans amplitudes of 59 ms (altered) and 32.2 ms (control). Percent changes were compared between methods and the amplitude of alternans to determine which method correlated better for each electro-physiological alteration.

Table 2, Amplitude of alternans. The percent change values were used to represent how stability changes for each electro-physiological alteration. Electro-physiological alterations that produced greater alternans amplitudes were considered to be less stable and those that produce lower alternans amplitudes were considered to be more stable.

	Alternans (ms)	% change from Control
Control	32.2	-
$I_{kr}*0.38$	59	83.2%
$I_{kr}*1.62$	0	-100.0%
$I_{k1}*0.93$	60	86.3%
$I_{k1}*1.07$	0	-100.0%
$I_{to}*0.9$	9.4	-70.8%
$I_{to}*1.1$	37.2	15.5%
$I_{CaL}*0.95$	0.2	-99.4%
$I_{CaL}*1.05$	49.2	52.8%
$I_{NaCa}*0.5$	43.2	34.2%
$I_{NaCa}*1.5$	0.2	-99.4%
CV*0.95	33.4	3.7%
CV*1.05	31.8	-1.2%

Table 3 shows the percent changes that resulted from each electro-physiological alteration for all three methods and the measure of stability. Indexes computed from the SGA method changed more sensitively and had larger percent changes than indexes computed from the two restitution methods. Percent changes of the SGA method and dynamic restitution had the same sign as percent changes of the amplitude of alternans for ten of the twelve electro-physiological alterations. Percent changes of standard restitution had the same sign as percent changes of the amplitude of alternans for nine of the twelve electro-physiological alterations. Percent changes were largest when altering I_{kr} and I_{k1} for dynamic and standard restitution methods and when I_{NaCa} was decreased by 50% for the SGA method. Altering I_{CaL} by 5% and I_{to} by 10% had comparatively larger effects for the SGA method than for dynamic and standard restitution methods.

Table 3, Percent changes of indexes computed from each method and the measure of stability. If an index computed from a method changed in a similar fashion to the amplitude of alternans, it was considered to correlate well. Percent changes in bold did not correlate well.

	Methods			Stability Measure
	Dynamic	Standard	SGA	Amplitude of Alternans
$I_{kr}*0.38$	7.0%	5.4%	**-10.1%**	83.2%
$I_{kr}*1.62$	-5.6%	-5.6%	-10.2%	-100.0%
$I_{k1}*0.93$	6.7%	5.3%	**-1.6%**	86.3%
$I_{k1}*1.07$	-6.6%	-6.0%	-21.2%	-100.0%
$I_{to}*0.9$	-0.7%	-1.0%	-23.4%	-70.8%
$I_{to}*1.1$	**-0.5%**	**-0.1%**	13.3%	15.5%
$I_{CaL}*0.95$	-4.4%	-3.3%	-23.7%	-99.4%
$I_{CaL}*1.05$	3.0%	2.2%	9.1%	52.8%
$I_{NaCa}*0.5$	2.1%	**-0.8%**	6.9%	34.2%
$I_{NaCa}*1.5$	-2.9%	-3.3%	-45.9%	-99.4%
CV*0.95	**-0.1%**	**-0.3%**	7.9%	3.7%
CV*1.05	-1.1%	-0.3%	-5.8%	-1.2%

The purpose of this study was to determine how well each method correlated with the amplitude of alternans for different electro-physiological alterations. The SGA method correlated better with changes in the amplitude of alternans than restitution methods when I_{to} and CV were decreased. Restitution methods correlated better with changes in the changes in the amplitude of alternans when repolarizing K^+ currents, I_{k1} and I_{kr}, were decreased. Standard restitution did not correlate well with the change in the amplitude of alternans when I_{NaCa} was decreased. Otherwise, restitution methods and the SGA method both correlated well with changes in the amplitude of alternans for all other electro-physiological alterations.

Figure 10 shows how each method fared when I_{kr} was altered. When I_{kr} was increased, each index decreased and all percent changes were negative, as shown in Table 3. When I_{kr} was decreased, the index computed from the SGA method decreased unlike indexes computed from dynamic and standard restitution shown in Figure 10B and Figure 10C. The amplitude of alternans, similar to dynamic and standard restitution, had a positive

percent change when I_{kr} was decreased. Figure 10D shows how much the index computed from the SGA method differed from indexes computed from dynamic restitution, standard restitution, and changes in the amplitude of alternans when I_{kr} was decreased. Figure 10A shows that the site at which APD alternans peaked moved further away from the pacing site when I_{kr} was decreased, which caused the index computed from the SGA method to decrease and the percent change to be negative.

A
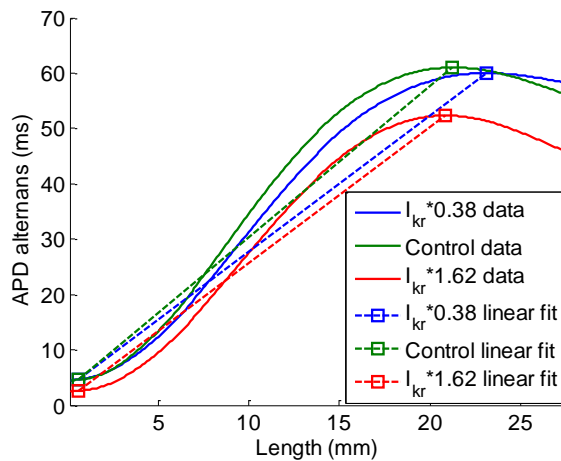
Figure 10, Altering I_{kr} by ±62% for (A) the SGA, (B) dynamic restitution, and (C) standard restitution. The dashed line in (B) and (C) represents constant CL at different values of APD and DI. The CL computed during control simulations is used to denote the constant CL line. Asterisks to the left of the constant CL line predict greater stability and asterisks to the right of the constant CL line predict less stability. (D) shows how much the index for each method changed when I_{kr} was decreased. Decreasing I_{kr} changed the index computed from the SGA by -10.1%, from 2.74 ms/mm to 2.46 ms/mm. Decreasing I_{kr} changed the index of dynamic restitution by 7% and standard restitution by 5.4%.

B

C

Figure 10, continued. Altering I_{kr} by ±62% for (A) the SGA, (B) dynamic restitution, and (C) standard restitution. The dashed line in (B) and (C) represents constant CL at different values of APD and DI. The CL computed during control simulations is used to denote the constant CL line. Asterisks to the left of the constant CL line predict greater stability and asterisks to the right of the constant CL line predict less stability. (D) shows how much the index for each method changed when I_{kr} was decreased. Decreasing I_{kr} changed the index computed from the SGA by -10.1%, from 2.74 ms/mm to 2.46 ms/mm. Decreasing I_{kr} changed the index of dynamic restitution by 7% and standard restitution by 5.4%.

D

Figure 10, continued. Altering I_{kr} by ±62% for (A) the SGA, (B) dynamic restitution, and (C) standard restitution. The dashed line in (B) and (C) represents constant CL at different values of APD and DI. The CL computed during control simulations is used to denote the constant CL line. Asterisks to the left of the constant CL line predict greater stability and asterisks to the right of the constant CL line predict less stability. (D) shows how much the index for each method changed when I_{kr} was decreased. Decreasing I_{kr} changed the index computed from the SGA by -10.1%, from 2.74 ms/mm to 2.46 ms/mm. Decreasing I_{kr} changed the index of dynamic restitution by 7% and standard restitution by 5.4%.

The index computed from the SGA correlated poorly with the change in the amplitude of alternans when I_{kr} was decreased. One difference between the SGA method and simulations used to compute the amplitude of alternans, is that the SGA method paced using a constant DI at the pacing site, while the simulations used to compute the amplitude of alternans paced using a constant CL at the pacing site. Though DI is controlled at a constant value at the pacing site in the SGA method, DI is not constant for consecutive beats at sites distal to the pacing site. Restitution set in at these distal sites and caused DI to oscillate similar to the way DI oscillates during CL control. When computing the amplitude of alternans, CL was fairly consistent throughout the tissue for

the same activation. The differences between using DI control or CL control were studied by computing restitution curves in a single cell using each method of pacing.

Figure 11A shows little difference between CL control and DI control when no electro-physiological alterations were performed. However, Figure 11B shows that values of APD were slightly less during CL control than during DI control for DIs between 30 ms and 60 ms when I_{kr} was decreased. Therefore, when DI started to oscillate at sites distal to the pacing site during DI control, APDs following longer DIs were shorter when I_{kr} was decreased than when no electro-physiological alterations were performed. These results help to show differences caused by using DI control and CL control for the methods used to predict changes in stability. When DI was controlled at a value of 35 ms, APD alternans decreased by 3.6 ms in the middle of the tissue when I_{kr} was decreased. When CL was controlled at a value of 200 ms, APD alternans increased by 26.8 ms in the middle of tissue when I_{kr} was decreased.

A
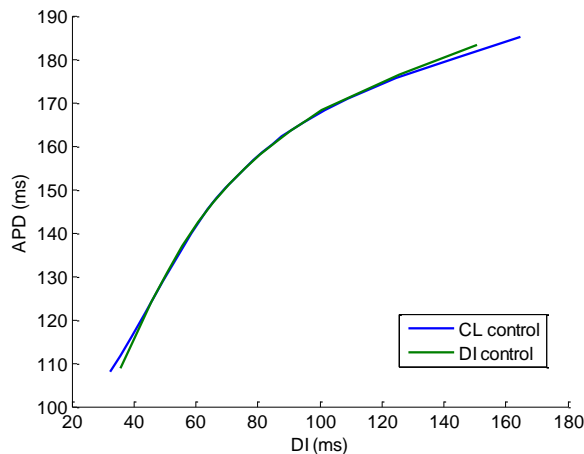
Figure 11, Restitution curves computed using DI control and CL control when (A) no electro-physiological alterations were performed and (B) when I_{kr} was decreased by 62%. Notice that (A) shows minimal difference between restitution curves computed from DI and CL control, while (B) shows that APD was higher (as much as 4 ms) during DI control than during CL control for DIs between 30 ms and 60 ms when I_{kr} was decreased by 62%.

B
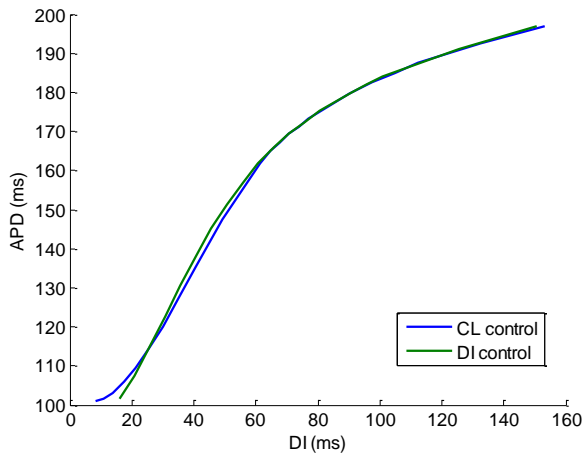
Figure 11, continued. Restitution curves computed using DI control and CL control when (A) no electro-physiological alterations were performed and (B) when I_{kr} was decreased by 62%. Notice that (A) shows minimal difference between restitution curves computed from DI and CL control, while (B) shows that APD was higher (as much as 4 ms) during DI control than during CL control for DIs between 30 ms and 60 ms when I_{kr} was decreased by 62%.

Figure 12 shows that indexes computed from dynamic and standard restitution changed minimally, but the index computed from the SGA changed substantially when I_{to} was altered. Figure 12 B and 12 C shows that the indexes computed from the two restitution methods decreased slightly when I_{to} was increased, which conflicts with changes in the amplitude of alternans and the index computed from the SGA method which increased when I_{to} was increased. At higher DIs, Figures 10 B and C and 12 B and C show that APD values change less when I_{to} is altered than when I_{kr} is altered. A reduced change in APD at high DIs reduced how much the index computed from restitution methods changed when I_{to} was altered.
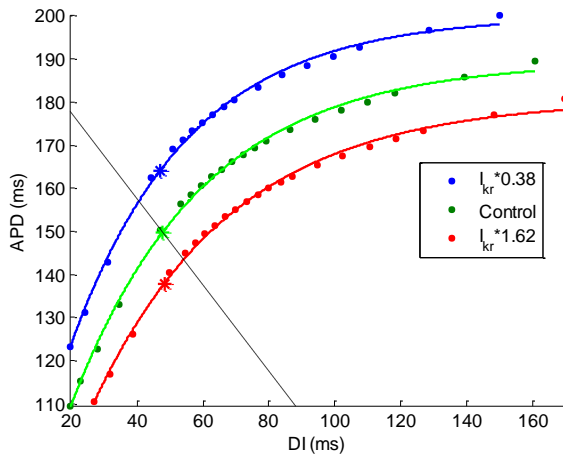
A
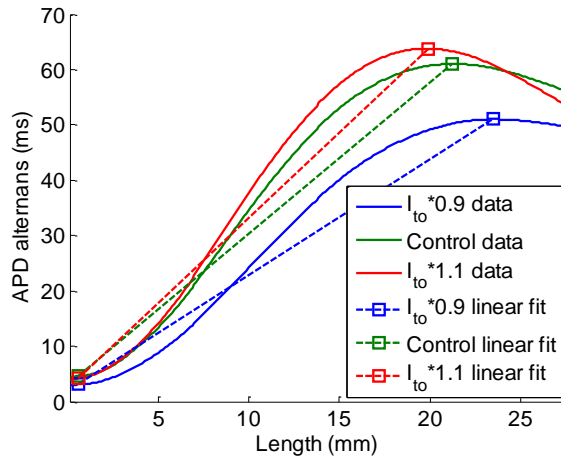
B
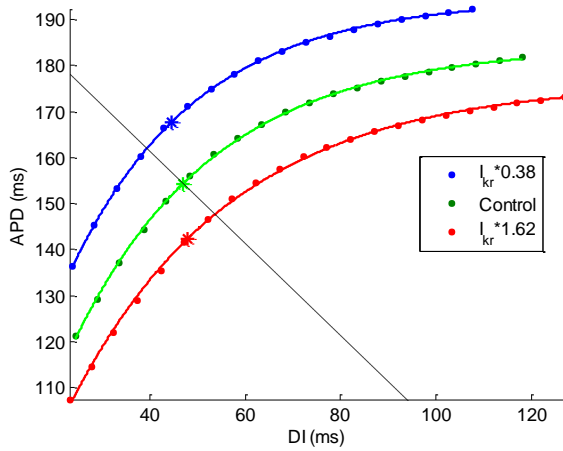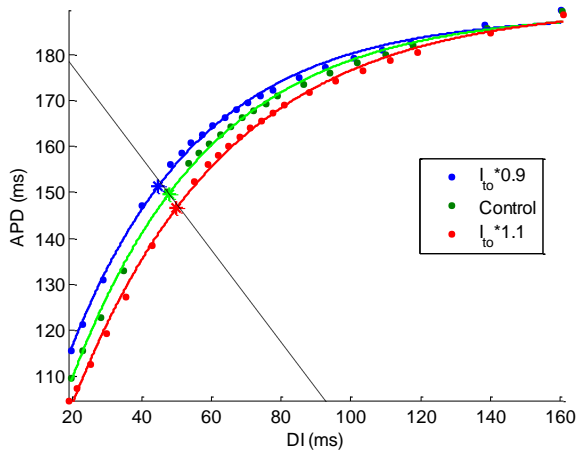

Figure 12, Altering I_{to} by $\pm 10\%$ for (A) the SGA, (B) dynamic restitution, and (C) standard restitution. Asterisks in (B) and (C) mark points where the slope approached +1 for each curve. (D) shows how much the index of each method changed when I_{to} was altered. Increasing I_{to} by 10% changed the index computed from the SGA by 13.3%, from 2.74 ms/mm to 3.10 ms/mm. Increasing I_{to} by 10% caused the indexes computed from dynamic and restitution to change minimally, by -0.5% and -0.1% respectively.
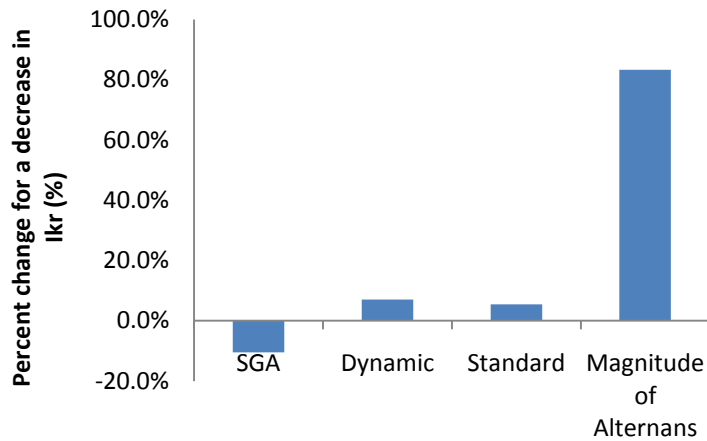
C
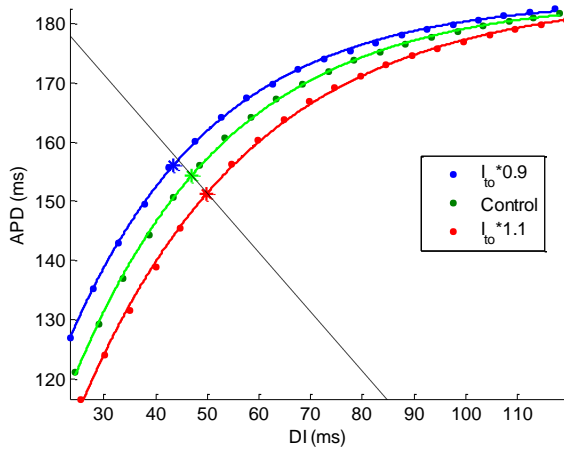
D
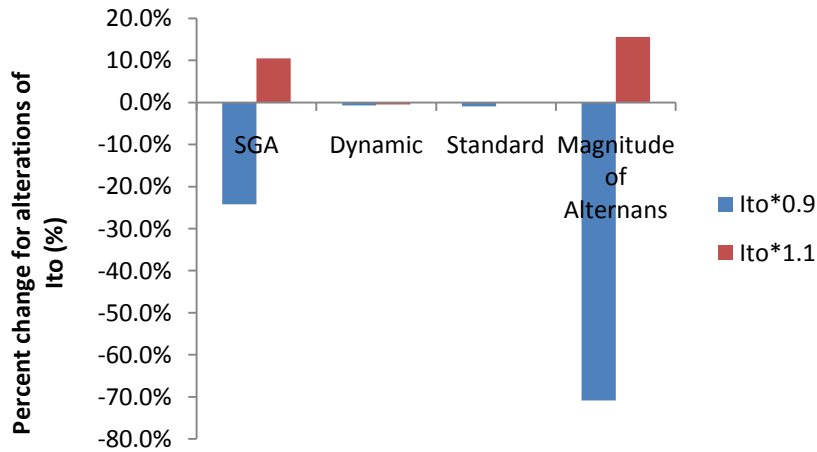
Figure 12, continued. Altering I_{to} by ±10% for (A) the SGA, (B) dynamic restitution, and (C) standard restitution. Asterisks in (B) and (C) mark points where the slope approached +1 for each curve. (D) shows how much the index of each method changed when I_{to} was altered. Increasing I_{to} by 10% changed the index computed from the SGA by 13.3%, from 2.74 ms/mm to 3.10 ms/mm. Increasing I_{to} by 10% caused the indexes computed from dynamic and restitution to change minimally, by -0.5% and -0.1% respectively.

Baseline APDs were computed at pacing CLs of 350 ms and 200 ms to explain the small change in APD at large values of DI when I_{to} was altered in Figures 12 B and C. As expected, increasing the amount of a repolarizing current (I_{k1}, I_{kr}, or I_{to}) or decreasing the amount of a depolarizing current (I_{CaL}) decreased APD for both pacing CLs. When I_{to} and I_{NaCa} were altered however, baseline APD changed substantially more when the pacing CL was 200 ms than when the pacing CL was 350 ms. These results are shown in Figure 13A and Figure 13B. Therefore, baseline APD changed differently when I_{to} and I_{NaCa} were altered at different cycle lengths. This changed the function fit to restitution curves in Figures 12 B and C and influenced the indexes computed from dynamic and standard restitution differently when I_{to} and I_{NaCa} were altered than when other electro-physiological alterations were made.

A
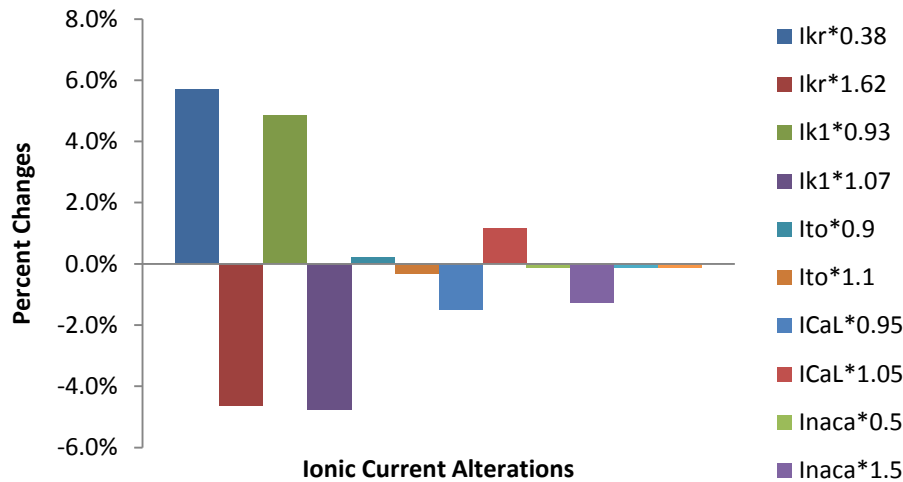
Figure 13, Baseline APDs for pacing CLs of (A) 350 ms and (B) 200 ms. Altering I_{to} and I_{NaCa} changed baseline APD more for the shorter CL.

B
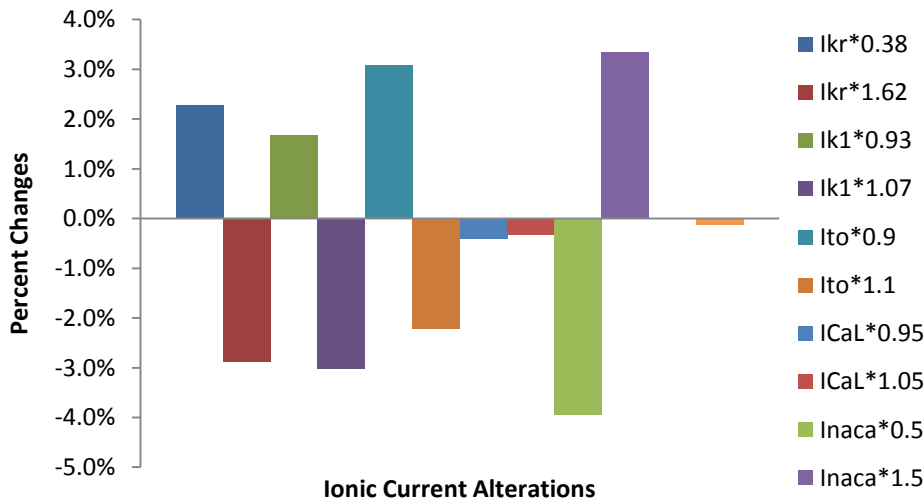
Figure 13, continued. Baseline APDs for pacing CLs of (A) 350 ms and (B) 200 ms. Altering I_{to} and I_{NaCa} changed baseline APD more for the shorter CL.

Figure 14 shows how altering CV affected the index computed from the SGA. Table 3 shows that indexes computed from dynamic and standard restitution and amplitude of alternans values changed minimally (less than 4%) when CV was altered. Decreasing CV by 5% changed the index computed from the SGA by 7.9%, from 2.74 ms/mm to 2.95 ms/mm. Increasing CV by 5% changed the index computed from the SGA by -5.8%, from 2.74 ms/mm to 2.58 ms/mm. Figure 14 shows that the index computed from the SGA method primarily changed when CV was altered because the site at which APD alternans peaked moved closer to or further away from the pacing site.
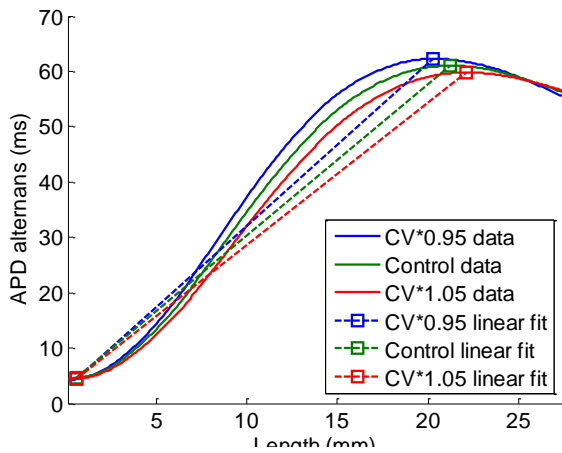
Figure 14, Alterations of CV by ±5% for the SGA. Increasing CV decreased the index computed from the SGA while decreasing CV increased the index.

Figure 15 shows that a relationship exists between the index computed from the SGA and the amount of APD alternans at the pacing site. Indexes computed from the SGA and the amount of APD alternans at the pacing site were computed for each electro-physiological alteration, including when DI was controlled at different values. A linear function, with an r^2 value of 0.69, best fit the points of all of the electro-physiological alterations. Altering I_{CaL} affected APD alternans at the pacing site more than any other ionic current alteration, while decreasing I_{kr} affected APD alternans at the pacing site the least of all ionic current alterations.
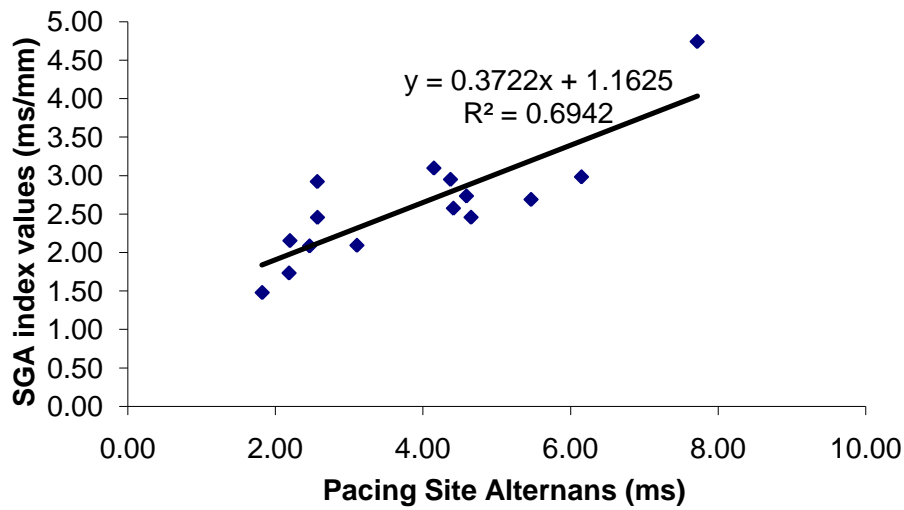
Figure 15, Indexes computed from the SGA were positively correlated with APD alternans at the pacing site and were fit linearly by the function $y = a * x + b$ where $y =$ SGA index, $x =$ APD alternans at the pacing site, $a = 0.372$, $b = 1.16$, and $r^2 = 0.69$.

Chapter Five: Discussion

A new method, the SGA method, is being proposed to predict cardiac electrical stability instead of restitution methods. In simulation, indexes of stability were computed from the SGA method and the restitution methods and then compared to changes in the amplitude of alternans for several different electro-physiological alterations. Results indicated that (1) restitution methods correlated better with changes in the amplitude of alternans when repolarizing K^+ currents, I_{kr} and I_{k1}, were decreased, (2) the SGA method correlated better with changes in the amplitude of alternans than restitution methods when I_{to} and CV were decreased, (3) standard restitution did not correlate as well with the change in the amplitude of alternans as dynamic restitution and the SGA method when I_{NaCa} was decreased, and (4) all three methods correlated well with changes in the amplitude of alternans for all other electro-physiological alterations.

The SGA method quantifies the component of DI dependent restitution and uses this to predict how stability will change for each electro-physiological alteration. The value of DI is controlled at the pacing site, but is lost for sites away from the pacing site. This causes alternation of DI and APD to incrementally increase for sites further away from the pacing site, shown in Figure 6C and 6D. This incremental increase of APD alternans along the length of the tissue was hypothesized to provide a more robust method of predicting stability than restitution methods, which predicts APD based on the previous DI in a single myocyte. Since APD is not solely a function of DI, the value of DI is controlled at a constant value at one end of the tissue and allowed to alternate at the other end of the tissue. The difference in APD alternans between the two ends of the tissue is proposed to provide a better measure of the contribution of DI on the following APD than the restitution curve.

Studies have shown that APD is not solely based on the previous DI, but also depends on other mechanisms such as memory [10, 11] and CV restitution [10, 30]. Furthermore, studies have shown that steep restitution does not predict arrhythmic activity [16, 19], and on a cellular level, does not always predict the occurrence of APD alternans [10, 31].

Values of APD can even alternate when DI is not alternating [20]. This finding has been verified by simulations within this study. Additionally, Saitoh et al. has shown that restitution does not correlate well with the magnitude of alternans in canine ventricular fibers [32]. Unlike restitution methods, the SGA method takes into account other effects besides APD restitution to predict cardiac electrical stability, such as spatial effects and CV restitution.

Different factors that affect stability, such as APD restitution and CV restitution, affect the morphology of SGA curves in different ways. As the slope of the APD restitution curve increases and APDs and DIs become shorter, alternans of APD and DI typically increases. Increasing alternans of APD and DI theoretically shifts the SGA curve vertically. In contrast, engaging CV restitution theoretically shifts the SGA curve horizontally. It has been proposed that steep CV restitution can change the position of APD nodes during discordant alternans [14]. Restitution of CV likely has a similar affect upon the SGA method, since both the node position and the SGA method depend upon how APD varies spatially. Figure 7 shows an example of the role CV restitution plays in the SGA method. In Figure 7, the site where APD alternans peaked in tissue shifted closer to the pacing site when the pacing interval was decreased from 35 ms to 30 ms and further away from the pacing site when the pacing interval was increased from 35 ms to 40 ms. If DI gradually decreases away from the pacing site, DI will eventually become short enough to engage CV restitution. Engaging CV restitution will reduce the CV of the wavefront. Reducing the CV of the wavefront does not allow DI to become so short that the wavefront collides with an earlier wavefront, which would result in conduction block. Reducing CV of this wavefront causes a gradual increase of DI along the 1-D strand. This gradual increase of DI engages APD restitution and causes a gradual increase in the following APD. As pacing intervals shorten and the slope of CV restitution increases, nodes move closer to the pacing site and the index used to compute the SGA method increases.

Changes in stability were measured using changes in the amplitude of alternans, which was selected since recent studies have proposed using the amplitude of TWA instead of a threshold to characterize electrical stability [33, 34]. Smith et al. developed a spectral

method to compute the amount of microvolt TWA of a patient [23] and a threshold of 1.9 µV is currently used for this method during exercise stress testing to determine whether a patient tests positive for T-wave alternans (TWA). Patients above this threshold of 1.9 µV are considered to test positive for TWA, while patients below this threshold are considered to test negative. The amplitude of TWA has been correlated with the onset of acute ischemia, acute volume overload, and ventricular fibrillation [35-37]. Using a quantitative measure of stability, such as the amplitude of alternans, may be an improvement over a measure of stability that uses a threshold, but it likely does not provide all prognostic information regarding cardiac electrical stability that other measures of stability may provide. Future studies should include other measures of stability besides the amplitude of alternans such as spiral wave breakup and if feasible, clinical studies, to measure cardiac electrical stability.

Table 3 shows that changes in the amplitude of alternans are much more sensitive to electro-physiological alterations and produce larger percent changes than any of the three methods. Percent changes of the two restitution methods are on average considerably less than percent changes produced by changes in the amplitude of alternans because altering an ionic current changes the value of APD alternans much more than the values of APD and DI for pacing CLs near 200 ms. Percent changes of changes in the amplitude of alternans are also on average larger than percent changes of the SGA method because of the way each is measured. The SGA method measures the rate of change of APD alternans in the tissue, which does not change as substantially as the amount of APD alternans at pacing CLs of 200 ms for any ionic current alteration.

The largest percent changes for the SGA method were produced by altering I_{NaCa}. Also, percent changes were comparatively larger for the SGA method than for restitution methods when I_{CaL} and I_{to} were altered. Large percent changes resulted when I_{NaCa}, I_{CaL}, and I_{to} were altered because of the model used in this study. The model used in this study was developed so that the amplitude of I_{CaL} and I_{NaCa} alternate at short pacing intervals (Figure 2 in Fox et al.) [27], which causes APD to alternate. The finding that alternating I_{CaL} causes APD to alternate is in agreement with other studies which suggest that calcium cycling is the underlying mechanism of repolarization alternans [18, 38].

The reason percent changes are larger for alterations of I_{NaCa} than I_{CaL} is that I_{NaCa} is altered by an order of magnitude more than I_{CaL}. These alteration magnitudes were chosen because these individual alterations, decreasing I_{NaCa} by 50% and decreasing I_{CaL} by 5%, eliminated alternans in single cell simulations. Altering I_{to} produced large percent changes for the SGA method because altering I_{to} has a large affect on the amount of I_{CaL} [39]. Altering I_{kr} doesn't affect percent changes of the SGA method as much as altering I_{CaL} since the model studied primarily uses alternation of I_{CaL} to cause APD alternans and I_{kr} has been suggested to alternate as a result of APD alternation [27]. Altering I_{kr} and I_{k1} did substantially affect the value of APD which affects the index computed from restitution methods. Restitution methods had the largest percent changes for alterations of I_{kr} and I_{k1}, since altering these ionic currents change the value of APD the most.

One interesting result was that the index computed from the SGA method decreased when repolarizing K+ currents, I_{kr} and I_{k1}, were decreased. Unlike the SGA method, decreasing I_{k1} and I_{kr} caused the index computed from restitution methods and the amplitude of APD alternans to increase. An increase in APD alternans is consistent with a study by Hua and Gilmour that shows a decrease in I_{kr} increased APD alternans in canines [40]. When K^+ repolarizing currents were decreased, APD alternans increased for methods that controlled CL at the pacing site, but not for the method that controlled DI at the pacing site.

Unlike the other methods, the SGA method controls DI at the pacing site. Since DI is no longer controlled at sites distal to the pacing site, APD and DI oscillate at these sites similar to CL control. Figure 11B shows a difference between a restitution curve computed using DI control and a restitution curve computed using CL control when I_{kr} was decreased. Figure 11B shows that APDs were shorter when CL is controlled than when DI is controlled for values of DI between 30 ms and 60 ms. Figure 11A shows no difference when no electro-physiological alterations are made.

Fox et al have suggested that I_{kr} alternates as a result of APD alternation [27]. Therefore, decreasing the amount of I_{kr} likely does not cause APD to alternate as much during DI control when DI is constant than during CL control when DI alternates. The shorter APD

is used for the restitution curve when APD bifurcates, which may explain why APD was shorter during CL control when I_{kr} was decreased. Changing between DI control and CL control changes the value of APD, even though the value of the previous DI is the same in both restitution curves. This demonstrates the importance of cardiac memory, where APD is not just based on the previous DI, but previous APDs and DIs as well [10].

There is a 30 ms to 60 ms range of DIs in which APDs were different between DI control and CL control pacing. This 30 ms to 60 ms range primarily consists of DIs larger than the 35 ms value, the value of DI that is controlled at the pacing site for the SGA method. The APD values occurring at these values of DI were typically the longer APDs used in the computation of APD alternans. Therefore, these longer APDs progressively decrease along the tissue and cause APD alternans to progressively decrease along the length of the tissue when I_{kr} is decreased. This progressive decrease of longer APDs along the tissue also increases the following shorter DI and shorter APD used in the computation of APD alternans. Both of these results cause the index computed from the SGA method to decrease when I_{kr} was decreased. The prediction of the SGA method that a decrease in I_{kr} will have a stabilizing effect contradicts studies that show proarrhythmia resulting from class III antiarrhythmic agents that block K^+ currents [41, 42].

The SGA method correlated better with changes in the amplitude of alternans than dynamic and standard restitution when I_{to} and I_{NaCa} were altered since baseline APD changed differently for different pacing CLs (Figure 13 A and B). Changing baseline APDs for different pacing CLs affected the indexes computed from the restitution methods. Figure 13 A and B show small percent changes in baseline APD for alterations of I_{to} and I_{NaCa} at a longer CL of 350 ms, but considerably larger percent changes in baseline APD for a shorter CL of 200 ms. This caused the point in each restitution curve where the slope approaches +1 to lie closer to the CL line, shown in Figure 12 B and C, which led to smaller values of percent change for restitution methods when I_{to} and I_{NaCa} were altered. In contrast, the index computed from the SGA method and the amplitude of alternans look at stability for only one pacing rate.

41

Using restitution methods may be misleading when baseline APD changes at different values of CL. If an electro-physiological alteration causes baseline APD to increase at long pacing CLs and decrease at short pacing CLs, the values of APD and DI at the point where the slope approaches +1 on a restitution curve would increase. This increase in APD and DI could increase the index computed from restitution above 215 ms, even though alternans may not occur during CLs much longer than 215 ms.

Another advantage of the SGA method is that it accounts for the effect of conduction throughout tissue, while restitution methods predict stability using only one site within the tissue. Accordingly, restitution methods did not correlate as well as the SGA method with changes in the amplitude of alternans when CV was decreased. The SGA predicted slower CV would have a destabilizing effect since a slower CV progressively increases DI for sites further away from the pacing site. APD restitution causes progressively longer APDs to follow these progressively longer DIs. This effect down the tissue leads to a progressive increase in APD alternans along the 1-D strand when CV is decreased.

It is interesting to note that the site where APD alternans peaked in Figure 14 shifted horizontally. When CV was decreased, the site where APD alternans peaked shifted closer to the pacing site. This horizontal shift in the site where APD alternans peaked is because decreasing CV caused DIs, and in turn APDs, to alternate progressively more along the tissue.

Conversely, the SGA method does not analyze the effect of a change in the pacing interval as well as restitution methods. Restitution methods show values of APD and DI at different pacing CLs, but SGA curves represent only one pacing interval. The index computed from the SGA method changed the most when the pacing rate was changed, which verified that the SGA method predicted a decrease in stability for faster pacing rates. The SGA method cannot be used for all pacing rates since pacing at values of DI much shorter than 30 ms resulted in 2:1 block at sites distal to the pacing site and pacing at values of DI much longer than 40 ms eliminates APD alternans throughout the tissue. When DI was controlled at 30 ms, CV restitution invoked discordant alternans, which has been shown to induce spiral wave breakup in simulated tissue [7].

Similar to controlling DI in the SGA method, Chrsitini et al. [43] has controlled alternans at a site and found that this decreases the spatial gradient of APD and suppresses discordant alternans in tissue. However, DI was controlled instead of CL at the pacing site in this study, which allowed for pacing at shorter values of CL without conduction block occurring. Pacing at a constant DI instead of a constant CL also suppressed APD alternans using the same CLs obtained from DI control. Figure 15 suggests that the amount of APD alternans at the pacing site is indicative of the amount of APD alternans in the rest of the tissue. This finding is similar to the study by Christini et al, since both found a potentially antiarrhythmic effect when APD alternans is decreased at the pacing site [43]. Alternans of APD at the pacing site changes differently for different electro-physiological alterations. In the model studied, APD alternans is primarily caused by I_{CaL} [27]. This relationship causes APD alternans at the pacing site to be dependent on I_{CaL}. The additional dependence of I_{CaL} on the previous DI [27] helps to explain the relationship between APD alternans at the pacing site and the index computed from the SGA method. As DI control is lost and DI alternation increases for sites further from the pacing site, I_{CaL} alternates more, which then causes APD to alternate more. Fox et al. have suggested that I_{kr} alternates as a result of APD alternation in the model studied [27], which explains why decreasing I_{kr} did not substantially change APD alternans at the pacing site. The relationship between APD alternans at the pacing site and the SGA method shows that determining the underlying affects of the DI independent mechanism of alternans is important in order to quantify the effect of the DI dependent mechanism of alternans.

Discrepancies exist between all of the methods studied and previous clinical studies. Reducing or blocking L-type calcium can have proarrhythmic affects, including the maintenance of atrial fibrillation [44, 45] and impairing excitation-contraction coupling [46, 47]. This result is inconsistent with all three methods and does not correlate well with changes in the amplitude of alternans. Therefore, other measures of stability are needed to predict different arrhythmic conditions.

A method has been presented that is based on the rate of change of the amplitude of alternans in tissue and then compared to other methods that are based on APD restitution.

Restitution methods do not incorporate other potentially proarrhythmic factors [10, 17, 18, 30], which suggests that a more robust method is needed to predict cardiac electrical stability. Restitution methods predict stability using a single myocyte, while the SGA method includes the effect of conduction throughout tissue. Restitution methods also base APD solely on the previous DI, without taking into effect cardiac memory, CV restitution, and other mechanisms that can affect stability.

Future studies should incorporate different measures of stability to compare against these methods used to predict stability. This study shows that the SGA method may be more effective than restitution protocols at predicting the effect some electro-physiological alterations have on alternans. If an ionic current that is causing cardiac electrical instability is diagnosed, the SGA method could help determine the drug that would be most effective to improve stability.

Chapter Six: Limitations

The main limitation of this study is that it is a simulation. The CVM model uses simplified modeling of both I_{CaL} and I_{to}. The CVM model also includes a simplified model of calcium cycling, including combining the calcium concentrations in the NSR and JSR. The ionic current I_{to} is comprised of two components, a fast and a slow component, but has been combined into one variable in this model [48]. A single cell has been found to couple to more than two other cells, making the linear strand used in the study not very relevant physiologically [49]. Spatially homogeneous models were simulated since spatial heterogeneities are complex and would have added a confounding factor in the interpretation of results.

Appendix 1

Parameters used in simulations:

Space Step, mm	0.125
Diffusion Coefficient, mm/s^2	0.07
Tissue Length, mm	31.25
Pacing Site, mm	0.625
	Min: 0.001
Time Step, ms	Max: 0.1

Alternative indexes to compute each method:

Other approaches can be used to compute indexes to predict changes in stability. The index computed from the SGA was computed as the slope of a fitted line from the pacing site to the site at which APD alternans peaked, as demonstrated in Figure 6D. The index computed from the SGA was also computed as the maximum slope of the low-pass filtered SGA curve. The maximum slope was computed as the two consecutive points in the SGA curve with the highest slope. Figure 16 shows the location of the maximum slope and plots a line containing the maximum slope computed from the SGA. Table 4 shows the results obtained when the index was computed as the maximum slope SGA curve. Computing the index of the SGA method using the maximum slope of the curve did not change the results substantially from when the index was computed using the slope of a fitted line.
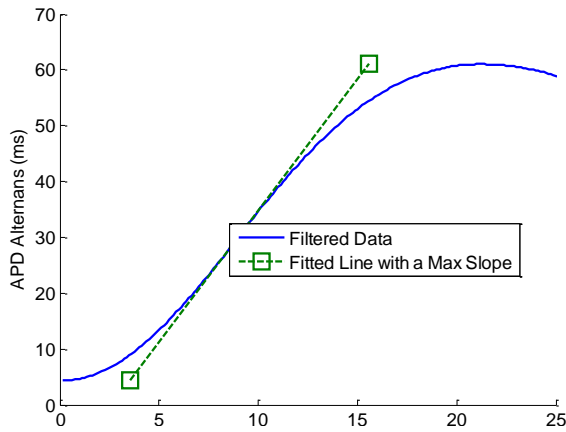
Figure 16, The maximum slope of the SGA method, which was considered to be used as an index for the SGA method.

Table 4, Values of the maximum slope computed from the SGA.

	Max Slope of the SGA (ms/mm)	% change from Control
Control	4.57	-
$I_{kr}*0.38$	4.09	-10.42%
$I_{kr}*1.62$	3.93	-14.00%
$I_{k1}*0.93$	4.47	-2.11%
$I_{k1}*1.07$	3.55	-22.41%
$I_{to}*0.9$	3.46	-24.23%
$I_{to}*1.1$	5.05	10.44%
$I_{CaL}*0.95$	3.45	-24.39%
$I_{CaL}*1.05$	5.06	10.85%
$I_{NaCa}*0.5$	4.55	-0.33%
$I_{NaCa}*1.5$	2.44	-46.59%
CV*0.95	4.85	6.09%
CV*1.05	4.34	-5.05%

Dynamic and standard restitution were computed by computing the APD and DI values when the slope approached +1 for an exponential function fit to the restitution curve. Since the measure of stability used was the amplitude of alternans during a pacing CL of 200 ms, an alternative index for both restitution methods was to compute the slope when the sum of APD and DI was closest to 200 ms on a fitted restitution curve, instead of computing the sum of APD and DI when the slope approached +1. Computing the index

using the slope when the sum of APD and DI was closest to 200 ms on a fitted restitution curve did not change the results substantially then when the index was computed using the sum of APD and DI when the slope approached +1. Table 5 and Table 6 show the values of slope when the sum of APD and DI were 200 ms.

Table 5, Indexes computed from the dynamic restitution method for each electro-physiological alteration when computing the sum of the APD and DI closest to 200 ms on a fitted restitution curve.

	Slope at APD+DI=200ms	% change from Control
Control	0.968	-
$I_{kr}*0.38$	1.165	20.36%
$I_{kr}*1.62$	0.846	-12.55%
$I_{k1}*0.93$	1.158	19.66%
$I_{k1}*1.07$	0.828	-14.41%
$I_{to}*0.9$	0.946	-2.23%
$I_{to}*1.1$	0.961	-0.65%
$I_{CaL}*0.95$	0.878	-9.22%
$I_{CaL}*1.05$	1.048	8.27%
$I_{NaCa}*0.5$	1.016	4.96%
$I_{NaCa}*1.5$	0.887	-8.31%
CV*0.95	0.964	-0.40%
CV*1.05	0.938	-3.08%

Table 6, Indexes computed from the standard restitution method for each electro-physiological alteration when computing the sum of the APD and DI closest to 200 ms on a fitted restitution curve.

	Slope at APD+DI=200ms	% change from Control
Control	1.023	-
I_{kr}*0.38	1.246	21.85%
I_{kr}*1.62	0.864	-15.54%
I_{k1}*0.93	1.232	20.51%
I_{k1}*1.07	0.848	-17.08%
I_{to}*0.9	0.991	-3.10%
I_{to}*1.1	1.016	-0.66%
I_{CaL}*0.95	0.920	-10.01%
I_{CaL}*1.05	1.106	8.19%
I_{NaCa}*0.5	0.996	-2.60%
I_{NaCa}*1.5	0.906	-11.36%
CV*0.95	1.013	-0.97%
CV*1.05	1.010	-1.20%

The minimum CL at which the onset of alternans occurred was originally used to measure stability instead of the amplitude of alternans at a pacing CL of 200 ms. The onset of APD alternans occurred when consecutive beats had absolute differences of ≥ 4 ms between APD values during steady state [18]. The dynamic restitution method had an unfair advantage over the other methods as it would commonly bifurcate near the point at which the slope was equal to unity. The bifurcation of the restitution curve, which demonstrates the onset of alternating behavior, caused the slope to increase more at this location than at other points along the curve. This bifurcation caused the onset of alternans to correlate strongly with the dynamic restitution method. The amplitude of alternans was later proposed and decided upon as a better measure of stability for this study. Table 7 and Figure 8 show the minimum CL at which the onset of alternans occurred in tissue for each electro-physiological alteration.

Table 7, The minimum CL at which the onset of alternans occurred for each electro-physiological alteration.

	Min CL (ms)	% change from Control
Control	204	-
$I_{kr}*0.38$	214	4.90%
$I_{kr}*1.62$	194	-4.90%
$I_{k1}*0.93$	214	4.90%
$I_{k1}*1.07$	192	-5.88%
$I_{to}*0.9$	200	-1.96%
$I_{to}*1.1$	208	1.96%
$I_{CaL}*0.95$	196	-3.92%
$I_{CaL}*1.05$	210	2.94%
$I_{NaCa}*0.5$	212	3.92%
$I_{NaCa}*1.5$	195	-4.41%
CV*0.95	205	0.49%
CV*1.05	204	0.00%
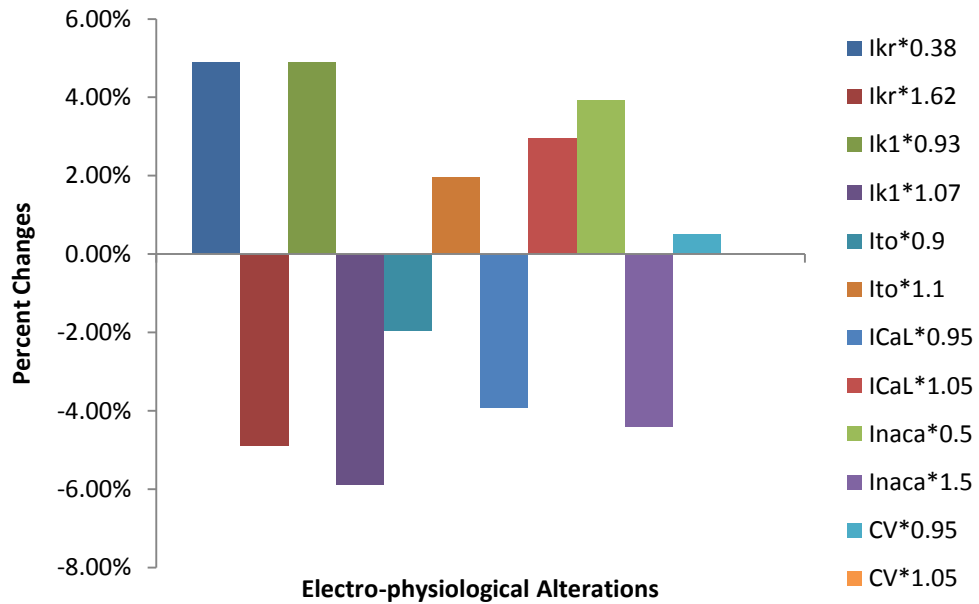
Figure 17, Percent changes of the onset of alternans for each electro-physiological alteration.

The Fenton-Karma model:

The Fenton-Karma (FK) model is a three variable model simulating action potentials of myocytes [28]. The FK model can be used to show the mechanism of the SGA since it can induce spatial variation of APD unlike many other cardiac cell models. Figure 18 shows an action potential modeled by the FK model. The FK model was not used because the CVM model more accurately represents the morphology of a cardiac action potential than the FK model. The FK model contains only three ionic currents compared to the 13 ionic currents of the CVM model. The three ionic currents represented in the FK model; Calcium, Potassium, and Sodium, are a simplified version of these currents and do not accurately portray their properties as well as the CVM model.
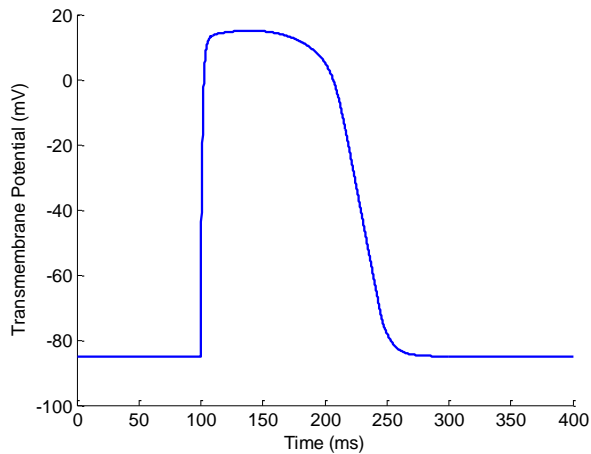
Figure 18, Simulated action potential of the FK model. Notice that the action potential of the FK model is not as complex as the action potential of the CVM model, shown in Figure 6A.

Figures and tables not included in the Results section:

Figures 19-22 show the results when I_{k1}, I_{CaL}, I_{NaCa}, and CV were altered, which were not shown in the Results section. Tables 8-10 list all of the index values computed from the SGA method, the dynamic restitution method, and the standard restitution method.

A
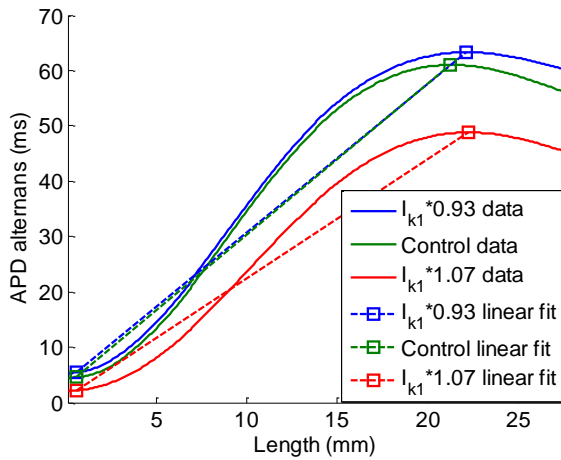
B
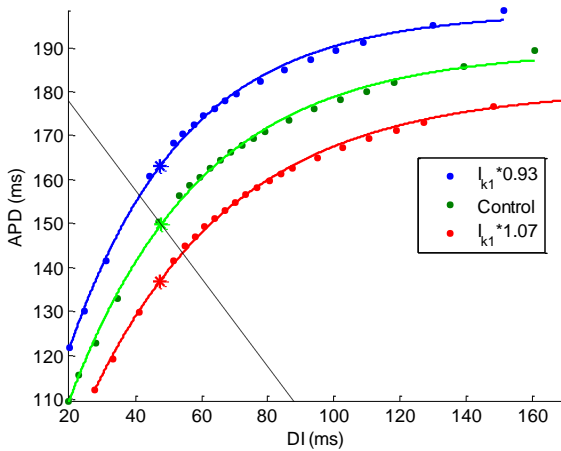
Figure 19, Altering I_{k1} by ±7% for (A) the SGA, (B) dynamic restitution, and (C) standard restitution.

C
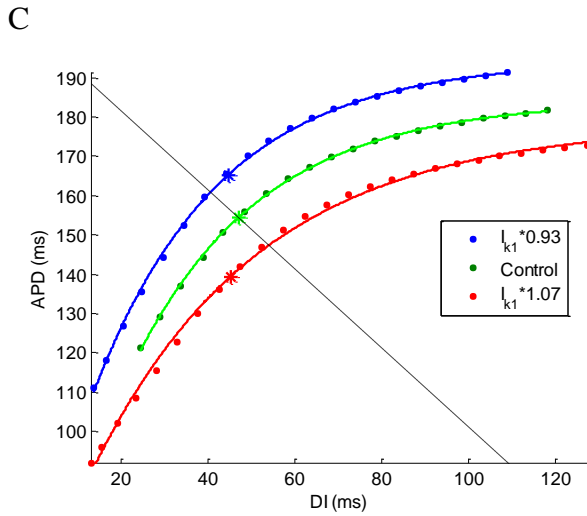
Figure 19, continued. Altering I_{k1} by ±7% for (A) the SGA, (B) dynamic restitution, and (C) standard restitution.

A
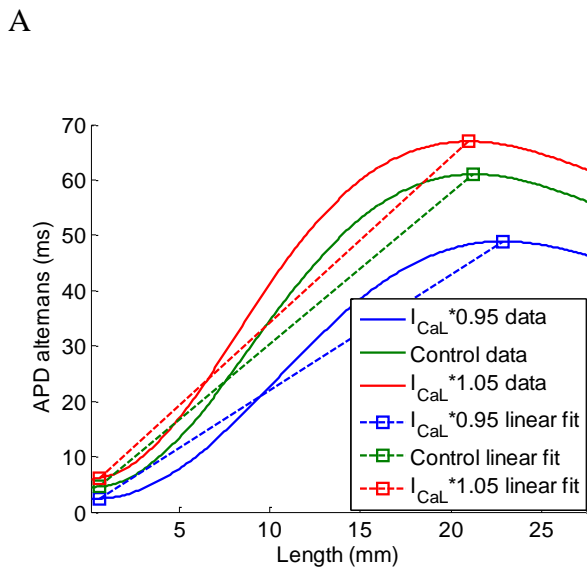
Figure 20, Altering I_{CaL} by ±5% for (A) the SGA, (B) dynamic restitution, and (C) standard restitution.

B
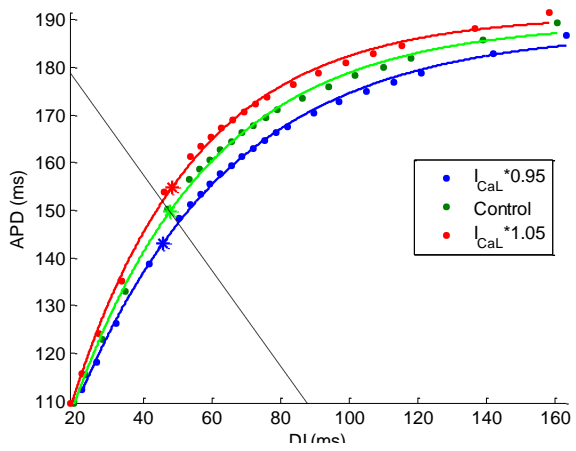
C
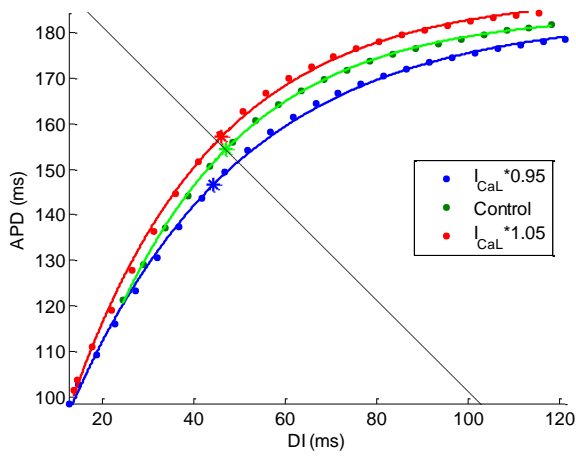
Figure 20, continued. Altering I_{CaL} by ±5% for (A) the SGA, (B) dynamic restitution, and (C) standard restitution

A
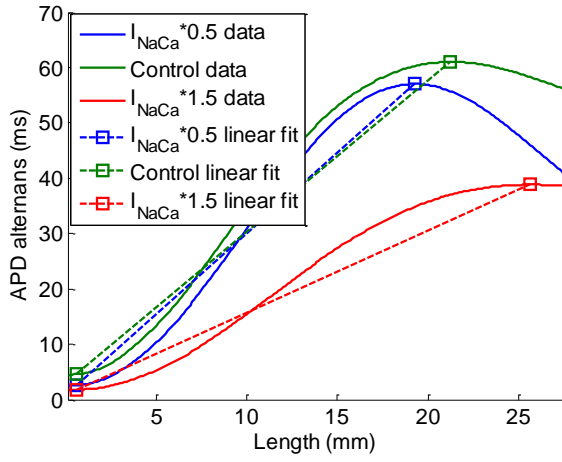
B
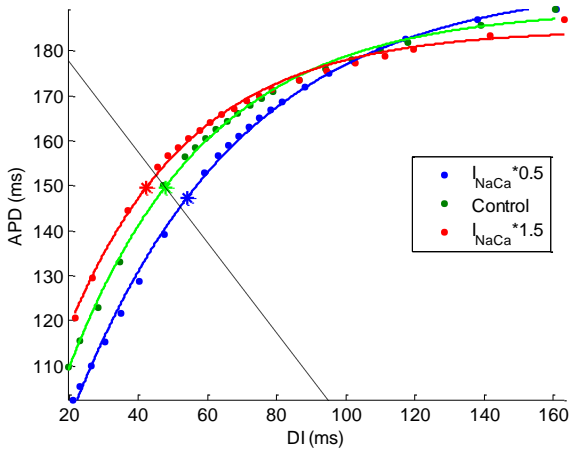
Figure 21, Altering I_{NaCa} by ±50% for (A) the SGA, (B) dynamic restitution, and (C) standard restitution.

C
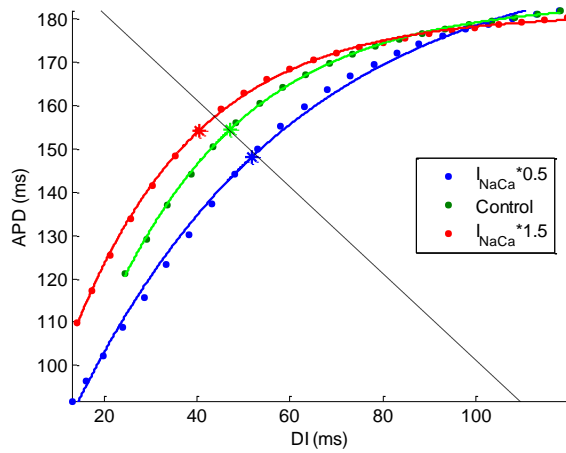
Figure 21, continued. Altering I_{NaCa} by ±50% for (A) the SGA, (B) dynamic restitution, and (C) standard restitution.

A
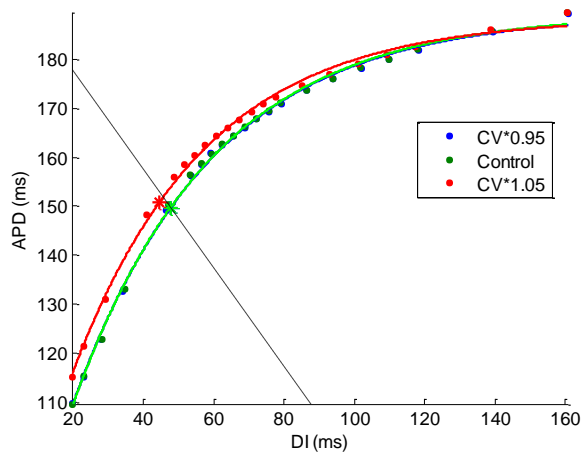
Figure 22, Altering CV by ±5% for (A) dynamic restitution, and (B) standard restitution.

B
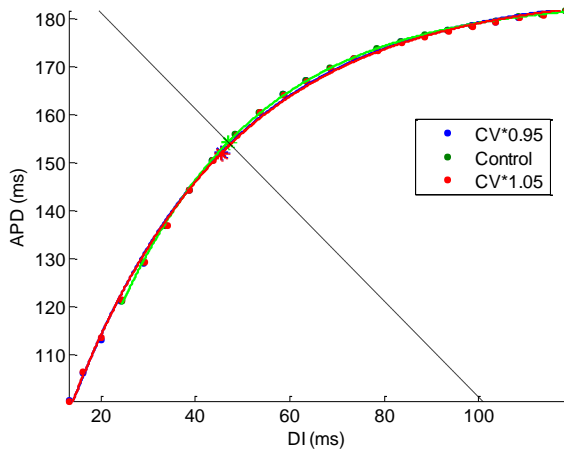
Figure 22, continued. Altering CV by ±5% for (A) dynamic restitution, and (B) standard restitution.

Table 8, Index values computed from the SGA method for all electro-physiological alterations.

	SGA index value (ms/mm)	% change from Control
Control	2.74	-
$I_{kr}*0.38$	2.46	-10.10%
$I_{kr}*1.62$	2.46	-10.16%
$I_{k1}*0.93$	2.69	-1.64%
$I_{k1}*1.07$	2.16	-21.20%
$I_{to}*0.9$	2.09	-23.44%
$I_{to}*1.1$	3.10	13.27%
$I_{CaL}*0.95$	2.09	-23.72%
$I_{CaL}*1.05$	2.98	9.08%
$I_{NaCa}*0.5$	2.92	6.87%
$I_{NaCa}*1.5$	1.48	-45.87%
CV*0.95	2.95	7.88%
CV*1.05	2.58	-5.82%

Table 9, Index values computed from the dynamic restitution method for all electro-physiological alterations. Values of APD and DI are listed when the slope approached +1 on the restitution curve for each alteration to show how indexes were computed.

	DI (ms)	APD (ms)	Index (ms)	% change from Control
Control	149.69	47.7	197.39	-
I_{kr}*0.38	164.15	47.1	211.25	7.02%
I_{kr}*1.62	137.94	48.3	186.24	-5.65%
I_{k1}*0.93	163.11	47.5	210.61	6.70%
I_{k1}*1.07	136.87	47.4	184.27	-6.65%
I_{to}*0.9	151.31	44.6	195.91	-0.75%
I_{to}*1.1	146.57	49.9	196.47	-0.47%
I_{CaL}*0.95	143.05	45.7	188.75	-4.38%
I_{CaL}*1.05	154.91	48.5	203.41	3.05%
I_{NaCa}*0.5	147.38	54.1	201.48	2.07%
I_{NaCa}*1.5	149.55	42.2	191.75	-2.86%
CV*0.95	149.51	47.6	197.11	-0.14%
CV*1.05	150.76	44.5	195.26	-1.08%

Table 10, Index values computed from the standard restitution method for all electro-physiological alterations. Values of APD and DI are listed when the slope approached +1 on the restitution curve for each alteration to show how indexes were computed.

	APD (ms)	DI (ms)	Index (ms)	% change from Control
Control	154.4	47.0	201.36	-
I_{kr}*0.38	167.7	44.6	212.31	5.44%
I_{kr}*1.62	142.3	47.9	190.18	-5.55%
I_{k1}*0.93	166.5	45.5	211.99	5.28%
I_{k1}*1.07	141.9	47.3	189.21	-6.03%
I_{to}*0.9	156.0	43.4	199.41	-0.97%
I_{to}*1.1	151.3	49.9	201.19	-0.08%
I_{CaL}*0.95	148.7	46.0	194.65	-3.33%
I_{CaL}*1.05	158.8	47.1	205.89	2.25%
I_{NaCa}*0.5	147.98	51.7	199.68	-0.83%
I_{NaCa}*1.5	154.27	40.5	194.77	-3.27%
CV*0.95	154.0	46.8	200.79	-0.28%
CV*1.05	153.8	46.9	200.74	-0.31%

Appendix 2

The Canine Ventricular Myocyte model:

The equations for the CVM model which was used in the study are listed below [27].

$$\frac{Dv}{Dt} = -(I_{stim} + I_{Na} + I_{K1} + I_{Kr} + I_{Ks} + I_{to} + I_{Kp} + I_{NaK} + I_{NaCa} + I_{Nab} + I_{Cab} + I_{pCa} + I_{Ca} + I_{CaK})$$

I_{stim} is the stimulus current given at the pacing site to initiate an action potential (-280 µA/µF for tissue and -80 µA/µF for a single cell).

Sodium current (I_{Na}):

$$I_{Na} = \overline{G}_{Na} * m^3 * h * j * (V - E_{Na})$$

$$\frac{dm}{dt} = \alpha_m(1 - m) - \beta_m * m$$

$$\frac{dh}{dt} = \alpha_h * (1 - h) - \beta_h * h$$

$$\frac{dj}{dt} = \alpha_j * (1 - j) - \beta_j * j$$

$$E_{Na} = \frac{RT}{F} * \ln\left(\frac{[Na^+]_o}{[Na^+]_i}\right)$$

$$\alpha_m = 0.32 * \frac{V + 47.13}{1 - e^{-0.1*(V+47.13)}}$$

$$\beta_m = 0.08 * e^{-V/11}$$

$$\alpha_h = 0.135 * e^{-(V+80)/6.8}$$

$$\beta_h = \frac{7.5}{1 + e^{-0.1*(V+11)}}$$

$$\alpha_j = \frac{0.175 e^{-(V+100)/23}}{1 + e^{0.15*(V+79)}}$$

$$\beta_j = \frac{0.3}{1 + e^{-0.1*(V+32)}}$$

Inward rectifier current (I_{K1}):

$$I_{K1} = \overline{G}_{K1} * K_1^\infty \frac{[K^+]_o}{[K^+]_o + K_{mK1}} * (V - E_K)$$

$$K_1^\infty = \frac{1}{2 + e^{\frac{1.62F}{RT}*(V-E_K)}}$$

$$E_K = \frac{RT}{F} * \ln\left(\frac{[K^+]_o}{[K^+]_i}\right)$$

Rapid component of the delayed rectifier K$^+$ current (I_{Kr}):

$$I_{Kr} = \overline{G}_{Kr} * R(V) * X_{Kr} * \sqrt{\frac{[K^+]_o}{4}} * (V - E_K)$$

$$\frac{dX_{Kr}}{dt} = \frac{X_{Kr}^\infty - X_{Kr}}{\tau_{Kr}}$$

$$R(V) = \frac{1}{1 + 2.5 * e^{0.1*(V+28)}}$$

$$\tau_{Kr} = 43 + \frac{1}{e^{-5.495+0.1691*V} + e^{-7.677-0.0128*V}}$$

$$X_{Kr}^{\infty} = \frac{1}{1 + e^{-2.182 - 0.1819*V}}$$

Slow component of the delayed rectifier K$^+$ current (I$_{Ks}$):

$$I_{Ks} = \overline{G}_{Ks} * X_{Ks}^2 * (V - E_{Ks}) \qquad\qquad E_{Ks} = \frac{RT}{F} * \ln\left(\frac{[K^+]_o + 0.01833 * [Na^+]_o}{[K^+]_i + 0.01833 * [Na^+]_i}\right)$$

$$\frac{dX_{Ks}}{dt} = \frac{X_{Ks}^{\infty} - X_{Ks}}{\tau_{Ks}} \qquad\qquad X_{Ks}^{\infty} = \frac{1}{1 + e^{-(V-16)/13.6}}$$

$$\tau_{Ks} = \frac{1}{\dfrac{0.0000719 * (V - 10)}{1 - e^{-0.148*(V-10)}} + \dfrac{0.000131 * (V - 10)}{e^{0.0687*(V-10)} - 1}}$$

Transient outward K$^+$ current (I$_{to}$):

$$I_{to} = \overline{G}_{to} * X_{to} * Y_{to} * (V - E_K) \qquad\qquad \frac{dX_{to}}{dt} = \alpha_{X_{to}}(1 - X_{to}) - \beta_{X_{to}} * X_{to}$$

$$\frac{dY_{to}}{dt} = \alpha_{Y_{to}}(1 - Y_{to}) - \beta_{Y_{to}} * Y_{to} \qquad\qquad \alpha_{X_{to}} = 0.04516 * e^{0.03577*V}$$

$$\beta_{X_{to}} = 0.0989 * e^{-0.06237*V} \qquad\qquad \alpha_{Y_{to}} = \frac{0.005415 * e^{-(V+33.5)/5}}{1 + 0.051335 * e^{-(V+33.5)/5}}$$

$$\beta_{Y_{to}} = \frac{0.005415 * e^{(V+33.5)/5}}{1 + 0.051335 * e^{(V+33.5)/5}}$$

Plateau K$^+$ current (I$_{Kp}$):

$$I_{Kp} = \overline{G}_{Kp} * K_{Kp} * (V - E_K) \qquad\qquad K_{Kp} = \frac{1}{1 + e^{(7.488-V)/5.98}}$$

Na$^+$-K$^+$ pump current (I$_{NaK}$):

$$I_{NaK} = \overline{I}_{NaK} * f_{NaK} * \frac{1}{1 + (\dfrac{K_{mNai}}{[Na^+]_i})^{1.5}} * \frac{[K^+]_o}{[K^+]_o + K_{mKo}}$$

$$f_{NaK} = \frac{1}{1 + 0.1245 * e^{-0.1*\frac{VF}{RT}} + 0.0365 * \sigma * e^{\frac{VF}{RT}}}$$

$$\sigma = \frac{1}{7} * (e^{\frac{[Na^+]_o}{67.3}} - 1)$$

Na$^+$/Ca^{2+} exchange current (I$_{NaCa}$):

$$I_{NaK} = \frac{k_{NaCa}}{K_{mNa}^3 + [Na^+]_o^3} * \frac{1}{K_{mCa} + [Ca^{2+}]_o} * \frac{1}{1 + k_{sat} * e^{\frac{V*F*(\eta-1)}{R*T}}} * \{e^{\frac{V*F*\eta}{R*T}} * [Na^+]_i^3$$

$$* [Ca^{2+}]_o - e^{\frac{V*F*(\eta-1)}{R*T}} * [Na^+]_o^3 * [Ca^{2+}]_i\}$$

Sarcolemmal pump current (I_{pCa}):

$$I_{pCa} = \overline{I}_{pCa} * \frac{[Ca^{2+}]_i}{K_{mpCa} + [Ca^{2+}]_i}$$

Ca^{2+} background current (I_{Cab}):

$$I_{Cab} = \overline{G}_{Cab} * (V - E_{Ca})$$

Na$^+$ background current (I_{Nab}):

$$I_{Nab} = \overline{G}_{Nab} * (V - E_{Na})$$

L-type Ca^{2+} channel current (I_{CaL}):

$$I_{CaL} = \overline{I}_{Ca} * f * d * f_{Ca}$$

$$\overline{I}_{Ca} = \frac{\overline{P}_{Ca}}{C_{sc}} * \frac{4 * V * F^2}{R * T} * \frac{[Ca^{2+}]_i * e^{2*V*F/R*T} - 0.341 * [Ca^{2+}]_o}{e^{2*V*F/R*T} - 1}$$

$$\frac{df}{dt} = \frac{f^\infty - f}{\tau_f} \qquad \frac{dd}{dt} = \frac{d^\infty - d}{\tau_d} \qquad \frac{df_{Ca}}{dt} = \frac{f_{Ca}^\infty - f_{Ca}}{\tau_{fCa}}$$

$$f^\infty = \frac{1}{1 + e^{(V+12.5)/5}} \qquad \tau_f = 30 + \frac{200}{1 + e^{(V+20)/9.5}}$$

$$d^\infty = \frac{1}{1 + e^{\frac{V+10}{-6.24}}} \qquad \tau_d = \frac{1}{\frac{0.25e^{-0.01*V}}{1 + e^{-0.07*V}} + \frac{0.07e^{-0.05*(V+40)}}{1 + e^{0.05*(V+40)}}}$$

$$f_{Ca}^\infty = \frac{1}{1 + (\frac{[Ca^{2+}]_i}{K_{mfCa}})^3}$$

K$^+$ current through the L-type Ca^{2+} channel (I_{CaK}):

$$I_{CaK} = \frac{\overline{P}_{CaK}}{C_{sc}} * \frac{f * d * f_{Ca}}{1 + \frac{\overline{I}_{Ca}}{I_{Cahalf}}} * \frac{1000 * V * F^2}{R * T} * \frac{[K^+]_i * e^{V*F/R*T} - [K^+]_o}{e^{V*F/R*T} - 1}$$

Glossary

T-Wave Alternans	TWA
Action Potential Duration	APD
Diastolic Interval	DI
Cycle Length	CL
Spatial Gradient of Alternans	SGA
Canine Ventricular Model	CVM
L-type Calcium Current	I_{CaL}
Transient Outward K^+ Current	I_{to}
Inward Rectifier K^+ Current	I_{k1}
Rapid Component of the Delayed Rectifier K^+ Current	I_{kr}
Na^+/Ca^{2+} Exchange Current	I_{NaCa}
Conduction Velocity	CV
Diffusion Coefficient	D_x
Transmembrane Potentials	TMP

References

1. Zheng, Z.J., et al., *Sudden cardiac death in the United States, 1989 to 1998.* Circulation, 2001. **104**(18): p. 2158-63.
2. Weiss, J.N., et al., *From pulsus to pulseless: the saga of cardiac alternans.* Circ Res, 2006. **98**(10): p. 1244-53.
3. Rosenbaum, D.S., et al., *Electrical alternans and vulnerability to ventricular arrhythmias.* N Engl J Med, 1994. **330**(4): p. 235-41.
4. Gehi, A.K., et al., *Microvolt T-wave alternans for the risk stratification of ventricular tachyarrhythmic events: a meta-analysis.* J Am Coll Cardiol, 2005. **46**(1): p. 75-82.
5. Nolasco, J.B. and R.W. Dahlen, *A graphic method for the study of alternation in cardiac action potentials.* J Appl Physiol, 1968. **25**(2): p. 191-6.
6. Karma, A., *Electrical alternans and spiral wave breakup in cardiac tissue.* Chaos, 1994. **4**(3): p. 461-472.
7. Fenton, F.H., et al., *Multiple mechanisms of spiral wave breakup in a model of cardiac electrical activity.* Chaos, 2002. **12**(3): p. 852-892.
8. Xie, F., et al., *Electrical refractory period restitution and spiral wave reentry in simulated cardiac tissue.* Am J Physiol Heart Circ Physiol, 2002. **283**(1): p. H448-60.
9. Koller, M.L., M.L. Riccio, and R.F. Gilmour, Jr., *Dynamic restitution of action potential duration during electrical alternans and ventricular fibrillation.* Am J Physiol, 1998. **275**(5 Pt 2): p. H1635-42.
10. Cherry, E.M. and F.H. Fenton, *Suppression of alternans and conduction blocks despite steep APD restitution: electrotonic, memory, and conduction velocity restitution effects.* Am J Physiol Heart Circ Physiol, 2004. **286**(6): p. H2332-41.
11. Fox, J.J., E. Bodenschatz, and R.F. Gilmour, Jr., *Period-doubling instability and memory in cardiac tissue.* Phys Rev Lett, 2002. **89**(13): p. 138101.
12. Tolkacheva, E.G., et al., *Condition for alternans and stability of the 1:1 response pattern in a "memory" model of paced cardiac dynamics.* Phys Rev E Stat Nonlin Soft Matter Phys, 2003. **67**(3 Pt 1): p. 031904.
13. Mironov, S., J. Jalife, and E.G. Tolkacheva, *Role of conduction velocity restitution and short-term memory in the development of action potential duration alternans in isolated rabbit hearts.* Circulation, 2008. **118**(1): p. 17-25.
14. Watanabe, M.A., et al., *Mechanisms for discordant alternans.* J Cardiovasc Electrophysiol, 2001. **12**(2): p. 196-206.
15. Pastore, J.M., et al., *Mechanism linking T-wave alternans to the genesis of cardiac fibrillation.* Circulation, 1999. **99**(10): p. 1385-94.
16. Banville, I., N. Chattipakorn, and R.A. Gray, *Restitution dynamics during pacing and arrhythmias in isolated pig hearts.* J Cardiovasc Electrophysiol, 2004. **15**(4): p. 455-63.
17. Huang, J., et al., *Restitution properties during ventricular fibrillation in the in situ swine heart.* Circulation, 2004. **110**(20): p. 3161-7.
18. Pruvot, E.J., et al., *Role of calcium cycling versus restitution in the mechanism of repolarization alternans.* Circ Res, 2004. **94**(8): p. 1083-90.

19. Narayan, S.M., et al., *T-wave alternans, restitution of human action potential duration, and outcome.* J Am Coll Cardiol, 2007. **50**(25): p. 2385-92.

20. Wu, R. and A. Patwardhan, *Mechanism of repolarization alternans has restitution of action potential duration dependent and independent components.* J Cardiovasc Electrophysiol, 2006. **17**(1): p. 87-93.

21. Wu, R. and A. Patwardhan, *Restitution of action potential duration during sequential changes in diastolic intervals shows multimodal behavior.* Circ Res, 2004. **94**(5): p. 634-41.

22. Kleber, A.G., et al., *Changes in conduction velocity during acute ischemia in ventricular myocardium of the isolated porcine heart.* Circulation, 1986. **73**(1): p. 189-98.

23. Smith, J.M., et al., *Electrical alternans and cardiac electrical instability.* Circulation, 1988. **77**(1): p. 110-21.

24. Bloomfield, D.M., S.H. Hohnloser, and R.J. Cohen, *Interpretation and classification of microvolt T wave alternans tests.* J Cardiovasc Electrophysiol, 2002. **13**(5): p. 502-12.

25. Mendez, C., C.C. Gruhzit, and G.K. Moe, *Influence of cycle length upon refractory period of auricles, ventricles, and A-V node in the dog.* Am J Physiol, 1956. **184**(2): p. 287-95.

26. Hodgkin, A.L., A.F. Huxley, and B. Katz, *Measurement of current-voltage relations in the membrane of the giant axon of Loligo.* J Physiol, 1952. **116**(4): p. 424-48.

27. Fox, J.J., J.L. McHarg, and R.F. Gilmour, Jr., *Ionic mechanism of electrical alternans.* Am J Physiol Heart Circ Physiol, 2002. **282**(2): p. H516-30.

28. Fenton, F. and A. Karma, *Vortex dynamics in three-dimensional continuous myocardium with fiber rotation: Filament instability and fibrillation.* Chaos, 1998. **8**(1): p. 20-47.

29. Cherry, E.M. and F.H. Fenton, *A tale of two dogs: analyzing two models of canine ventricular electrophysiology.* Am J Physiol Heart Circ Physiol, 2007. **292**(1): p. H43-55.

30. Banville, I. and R.A. Gray, *Effect of action potential duration and conduction velocity restitution and their spatial dispersion on alternans and the stability of arrhythmias.* J Cardiovasc Electrophysiol, 2002. **13**(11): p. 1141-9.

31. Hall, G.M., S. Bahar, and D.J. Gauthier, *Prevalence of rate-dependent behaviors in cardiac muscle.* Physical Review Letters, 1999. **82**(14): p. 2995-2998.

32. Saitoh, H., J.C. Bailey, and B. Surawicz, *Action potential duration alternans in dog Purkinje and ventricular muscle fibers. Further evidence in support of two different mechanisms.* Circulation, 1989. **80**(5): p. 1421-31.

33. Verrier, R.L., et al., *T-wave alternans: does size matter.* J Cardiovasc Electrophysiol, 2005. **16**(6): p. 625-8.

34. Klingenheben, T., P. Ptaszynski, and S.H. Hohnloser, *Quantitative assessment of microvolt T-wave alternans in patients with congestive heart failure.* J Cardiovasc Electrophysiol, 2005. **16**(6): p. 620-4.

35. Martinez, J.P., et al., *Characterization of repolarization alternans during ischemia: time-course and spatial analysis.* IEEE Trans Biomed Eng, 2006. **53**(4): p. 701-11.

36. Nearing, B.D. and R.L. Verrier, *Progressive increases in complexity of T-wave oscillations herald ischemia-induced ventricular fibrillation.* Circ Res, 2002. **91**(8): p. 727-32.

37. Narayan, S.M., et al., *Acute volume overload elevates T-wave alternans magnitude.* J Appl Physiol, 2007. **102**(4): p. 1462-8.

38. Walker, M.L. and D.S. Rosenbaum, *Repolarization alternans: implications for the mechanism and prevention of sudden cardiac death.* Cardiovasc Res, 2003. **57**(3): p. 599-614.

39. Greenstein, J.L., et al., *Role of the calcium-independent transient outward current I(to1) in shaping action potential morphology and duration.* Circ Res, 2000. **87**(11): p. 1026-33.

40. Hua, F. and R.F. Gilmour, Jr., *Contribution of IKr to rate-dependent action potential dynamics in canine endocardium.* Circ Res, 2004. **94**(6): p. 810-9.

41. Hondeghem, L.M. and D.J. Snyders, *Class III antiarrhythmic agents have a lot of potential but a long way to go. Reduced effectiveness and dangers of reverse use dependence.* Circulation, 1990. **81**(2): p. 686-90.

42. Brooks, R.R., et al., *Proarrhythmia of azimilide and other class III antiarrhythmic agents in the adrenergically stimulated rabbit.* Proc Soc Exp Biol Med, 2000. **223**(2): p. 183-9.

43. Christini, D.J., et al., *Control of electrical alternans in canine cardiac purkinje fibers.* Phys Rev Lett, 2006. **96**(10): p. 104101.

44. Lee, S.H., et al., *Effect of verapamil on long-term tachycardia-induced atrial electrical remodeling.* Circulation, 2000. **101**(2): p. 200-6.

45. Benardeau, A., S. Fareh, and S. Nattel, *Effects of verapamil on atrial fibrillation and its electrophysiological determinants in dogs.* Cardiovasc Res, 2001. **50**(1): p. 85-96.

46. Bers, D.M., *Cardiac excitation-contraction coupling.* Nature, 2002. **415**(6868): p. 198-205.

47. Mahajan, A., et al., *Modifying L-type calcium current kinetics: consequences for cardiac excitation and arrhythmia dynamics.* Biophys J, 2008. **94**(2): p. 411-23.

48. Grandi, E., F.S. Pasqualini, and D.M. Bers, *A novel computational model of the human ventricular action potential and Ca transient.* J Mol Cell Cardiol, 2009.

49. Saffitz, J.E., et al., *Tissue-specific determinants of anisotropic conduction velocity in canine atrial and ventricular myocardium.* Circ Res, 1994. **74**(6): p. 1065-70.

VITA

STUART TRAXEL

Date of Birth: March 14, 1984 in
Maysville, Ky

Degree Awarded

Bachelors of Science in Electrical Engineering

University of Kentucky, May 2007